FAME Observing Geometry and Mission Astrometric Errors

Marc A. Murison

Astronomical Applications Department
U.S. Naval Observatory
Washington, DC

December 20, 2000

Launch and GTO Configurations

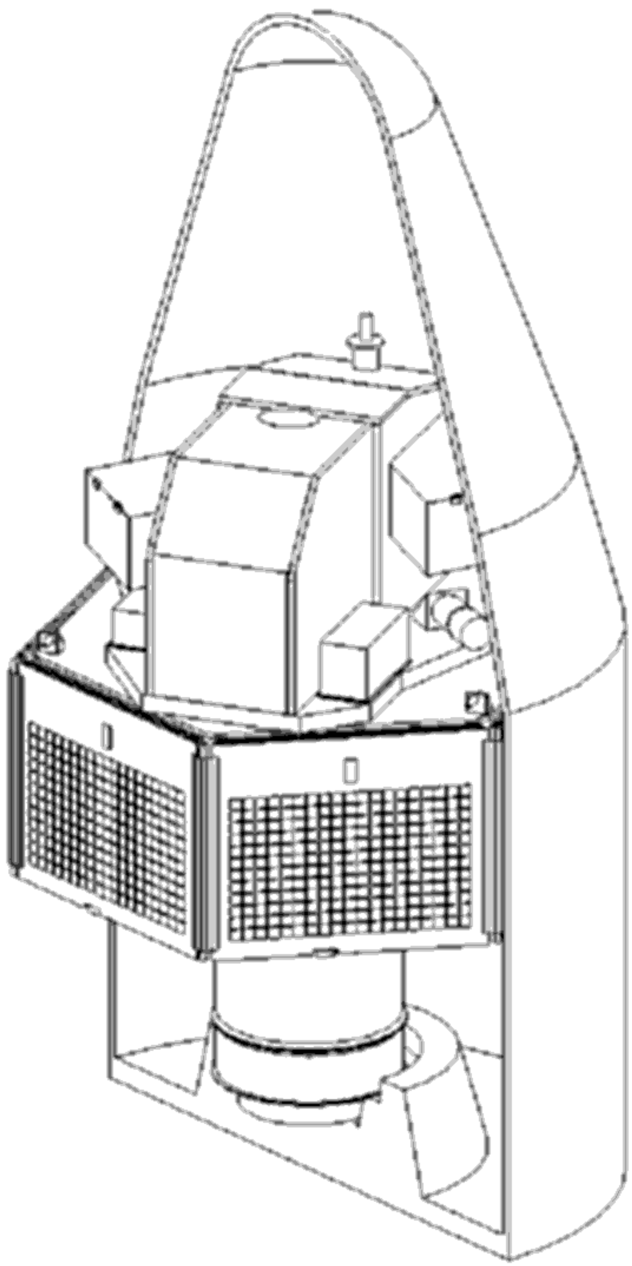

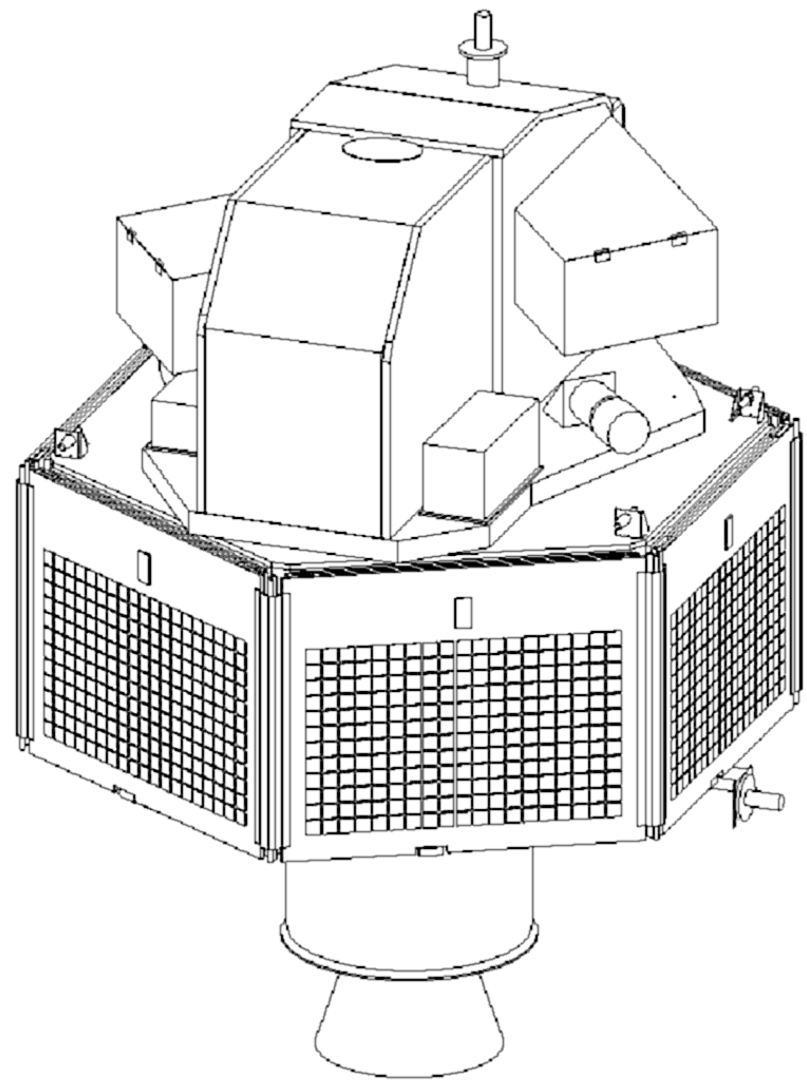

Operational Configuration

- High degree of symmetry
- Solar shield
  - thermal protection
  - electrical power
  - precession torque
    - steady (well, mostly)
    - very little ne
    - it's a freebie
  - "trim tabs"

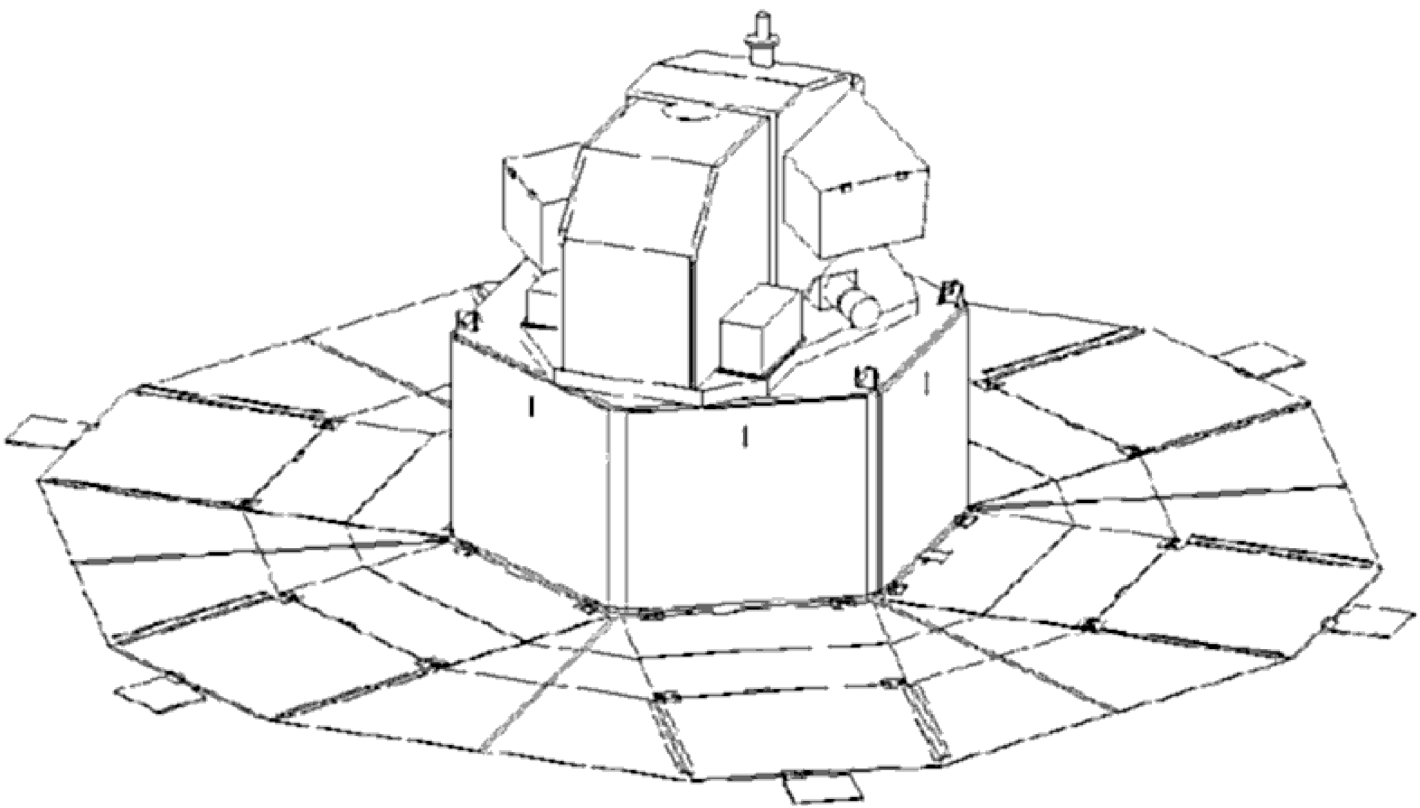

Choose Your Napping Time

- What determines mission accuracies?
  - the Great Divide: single-measurement errors and mission-averaged errors
- The heart of everything: geometry
  - how the instrument scans the sky
  - scan angle and observation density distributions
- Round and round we go: simulations
  - optimize the Sun angle, the spin period, and the precession period
  - all-sky density maps
  - histograms

Act I. What determines mission accuracies?

What Determines Mission Accuracies?

- Broadly speaking, we have "global" and "local" considerations
- Local
  - instrumental parameters and characteristics
  - detailed dynamical and orbital motions
  - this category contains all the physics
  - affects single-measurement accuracies
  - subject of another talk
- Global
  - driven entirely by the scanning geometry
  - two important distributions
    - distribution of observation density (a function of position on the sky)
    - distribution of scan angles (also a function of sky position)
      - scan angle: at a given point on the sky, the angle that the telescope FOV motion makes wrt an ecliptic meridian through that point
  - sets **upper bounds** on the mission-averaged accuracies that the instrument can achieve, given
    - the instrument geometry
    - a statistical description of the single-measurement errors

What Determines Mission Accuracies?

- nitty-gritties contribute to single-measurement errors ("local")
- observation density and scan angle distributions determined by scan geometry ("global")

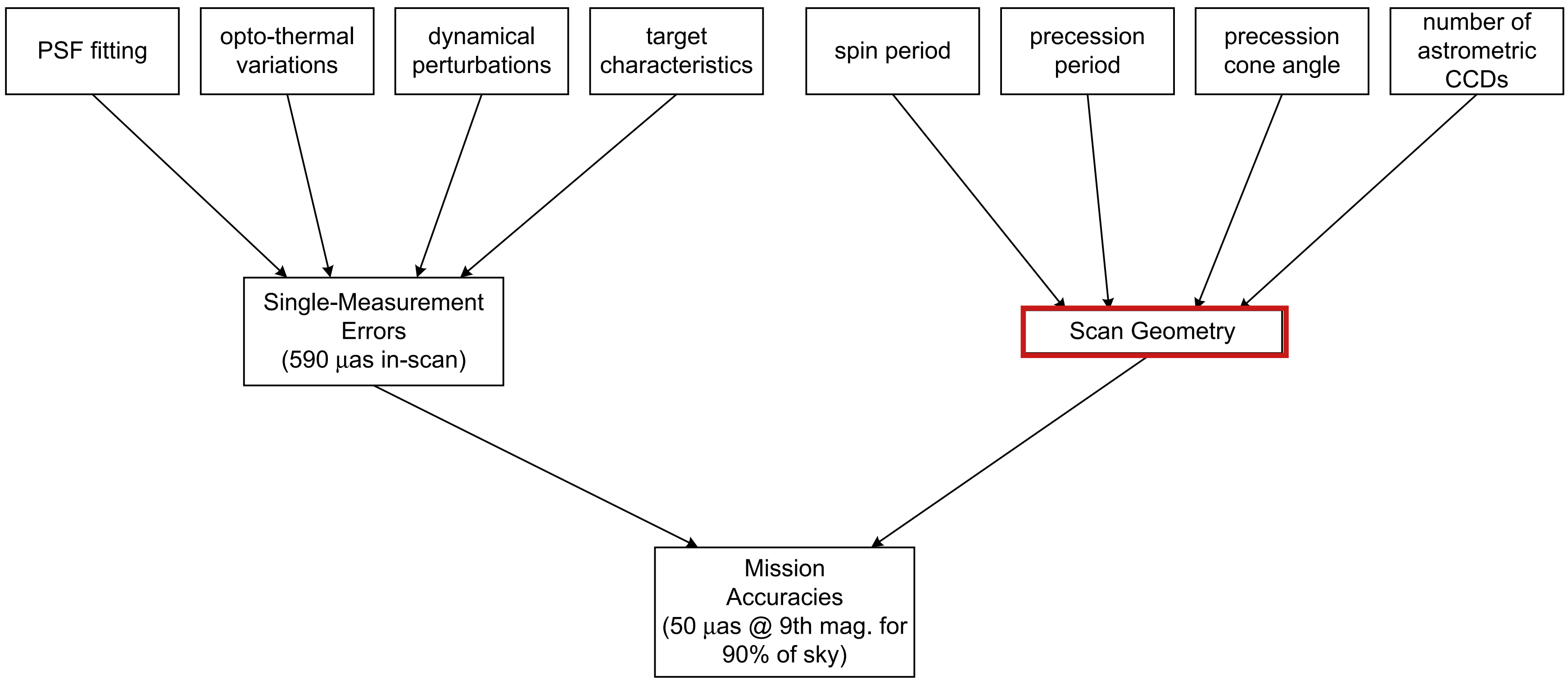

Act II. Geometry

Geometry

- Two distributions fundamentally affect the mission astrometric errors
  - Distribution of observations on the sky
  - Distribution of scan angle
    - angle between instantaneous scan direction and a local ecliptic meridian
    - determines orientation and ratio of error ellipse axes
- Ideally, both of these distributions should be
  - dense
  - homogeneous
- Intuitively, the distribution homogeneity depends on
  - Length of mission
  - Sun angle
  - Spin period
  - Precession rate

Geometry *(cont.)*

- Basic scanning geometry
  - fast spin (40 minutes) about the spacecraft symmetry axis
  - slow precession (20 days) of symmetry axis about nominal Sun direction
  - two viewports separated by the *basic angle* γ define the *observation plane*

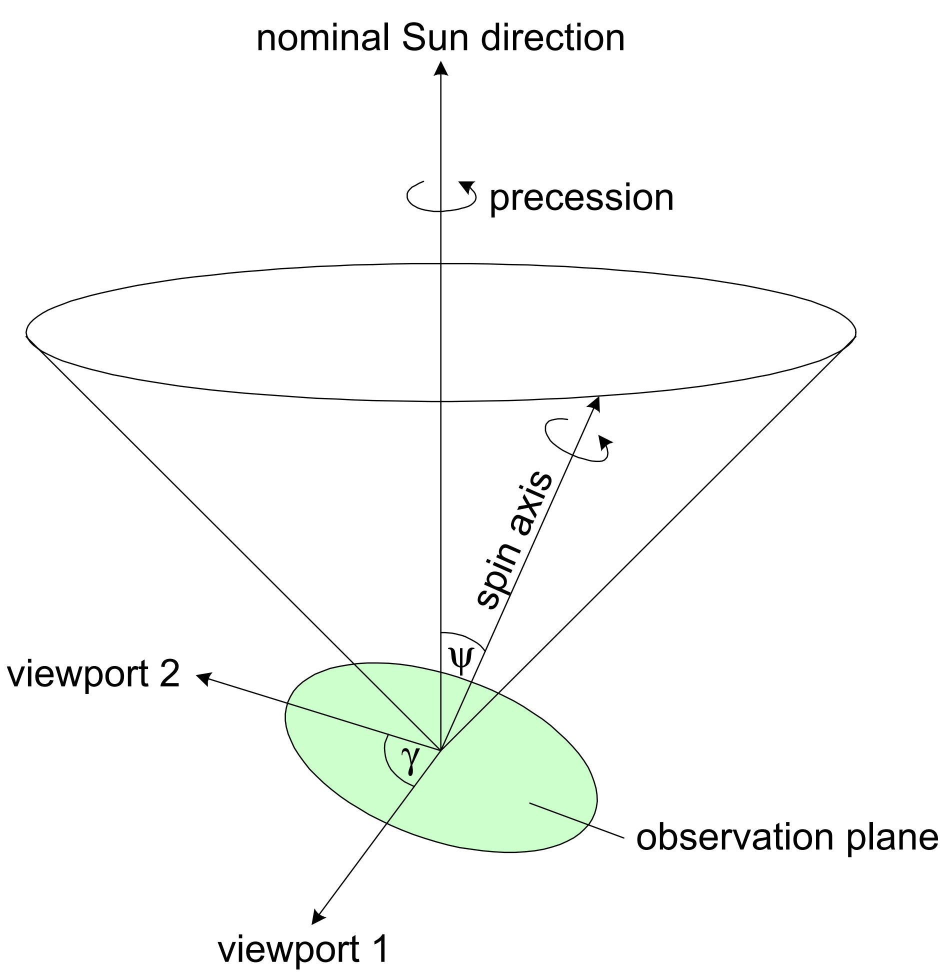

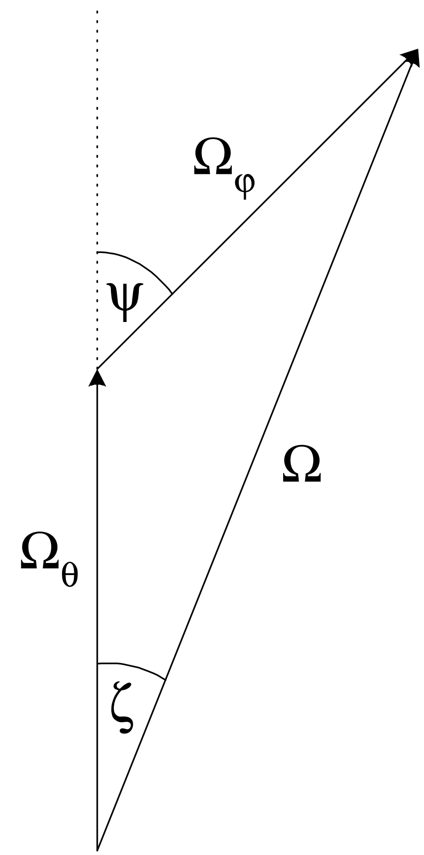

$$\tan\zeta = \frac{\Omega_\varphi \sin\psi}{\Omega_\theta + \Omega_\varphi \cos\psi} = \frac{\Omega_\varphi}{\Omega_\theta}\sin\psi + \left(\frac{\Omega_\varphi}{\Omega_\theta}\right)^2 \sin\psi\cos\psi + O\left[\left(\frac{\Omega_\varphi}{\Omega_\theta}\right)^3\right]$$

Geometry *(cont.)*

- Body frame [x,y,z] and "external" frame [X,Y,Z] linkage via Euler angles

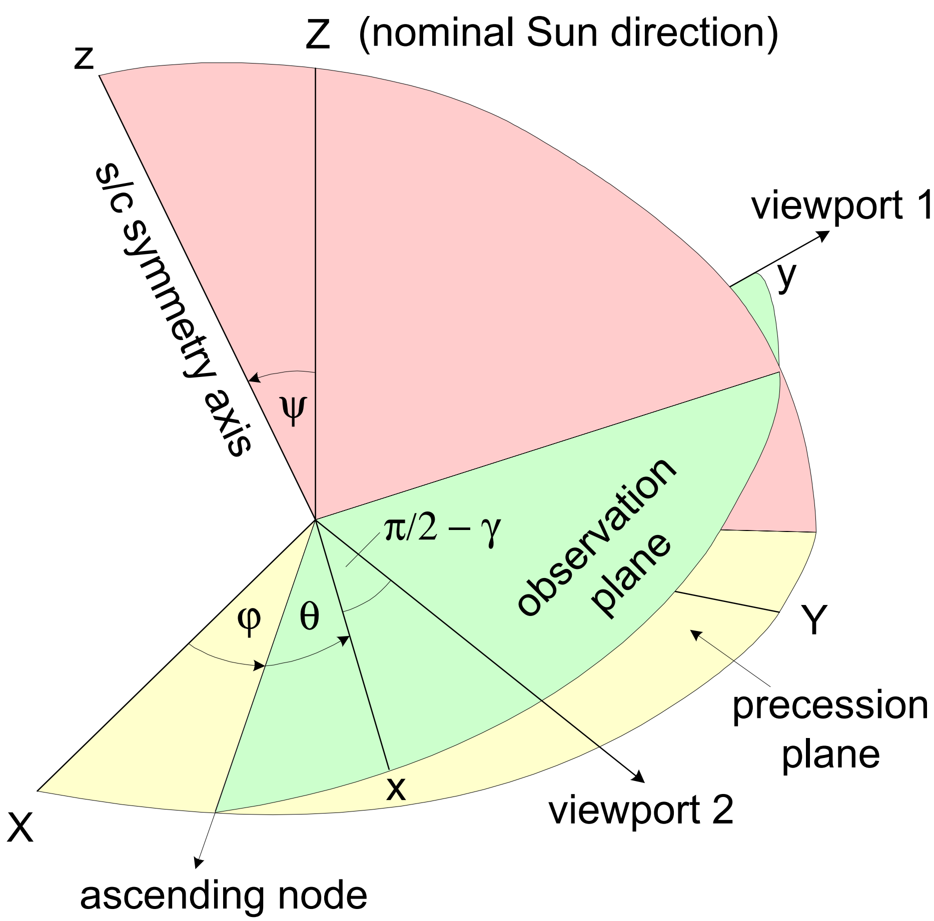

- Spherical geometry

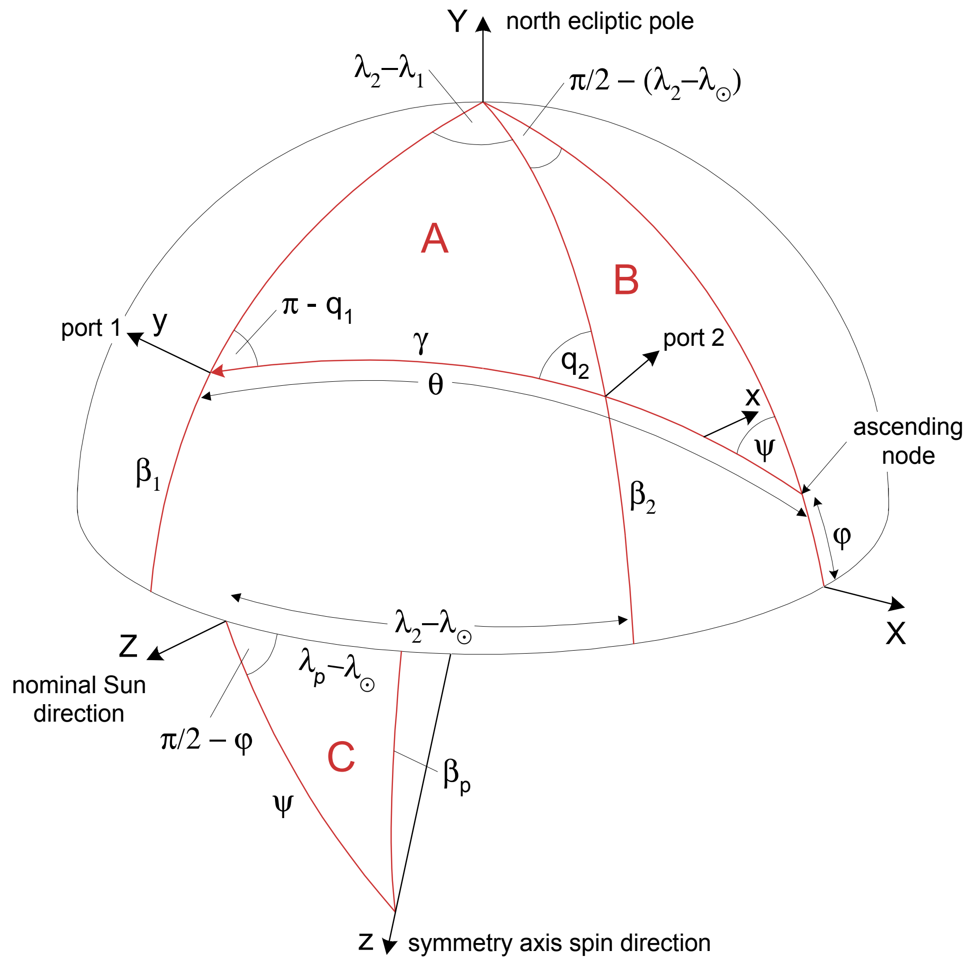

Geometry *(cont.)*

- Equations derived from the geometry and that describe the scan behavior: not hideous, but not trivial, either
- Ecliptic coordinates of viewport (as a function of spin phase θ, precession phase φ, precession cone angle ψ, and solar longitude):

$$\sin\beta_1 = \sin\phi\cos\theta + \cos\phi\sin\theta\cos\psi$$

$$\cos\lambda_1 = \frac{\sin\theta\sin\psi\cos\lambda_\odot + (\cos\psi\sin\theta\sin\phi - \cos\theta\cos\phi)\sin\lambda_\odot}{\sqrt{1-(\sin\phi\cos\theta + \cos\phi\sin\theta\cos\psi)^2}}$$

$$\sin\lambda_1 = \frac{\sin\theta\sin\psi\sin\lambda_\odot - (\cos\psi\sin\theta\sin\phi - \cos\theta\cos\phi)\cos\lambda_\odot}{\sqrt{1-(\sin\phi\cos\theta + \cos\phi\sin\theta\cos\psi)^2}}$$

- Scan angle (as a function of viewport location on the sky):

$$\sin q = Q \qquad \cos q = \frac{[\sin^2(\lambda-\lambda_\odot) - \cos^2(\lambda-\lambda_\odot)\sin^2\beta]\cos\psi + \frac{1}{Q}[\cos^2(\lambda-\lambda_\odot) - \sin^2\psi]\cos(\lambda-\lambda_\odot)\sin\beta}{\sin(\lambda-\lambda_\odot)[1-\cos^2(\lambda-\lambda_\odot)\cos^2\beta]}$$

where

$$Q = \frac{\cos(\lambda-\lambda_\odot)\cos\psi\sin\beta \pm |\sin(\lambda-\lambda_\odot)|\sqrt{\sin^2\psi - \cos^2(\lambda-\lambda_\odot)\cos^2\beta}}{1-\cos^2(\lambda-\lambda_\odot)\cos^2\beta}$$

Geometry *(cont.)*

- Precession cone "holes" in Sun and anti-Sun directions
  - hole boundaries determined by sqrt term of Q going imaginary
  - hole angular radius = 90 deg - Sun angle
  - immediate result: larger Sun angle is better

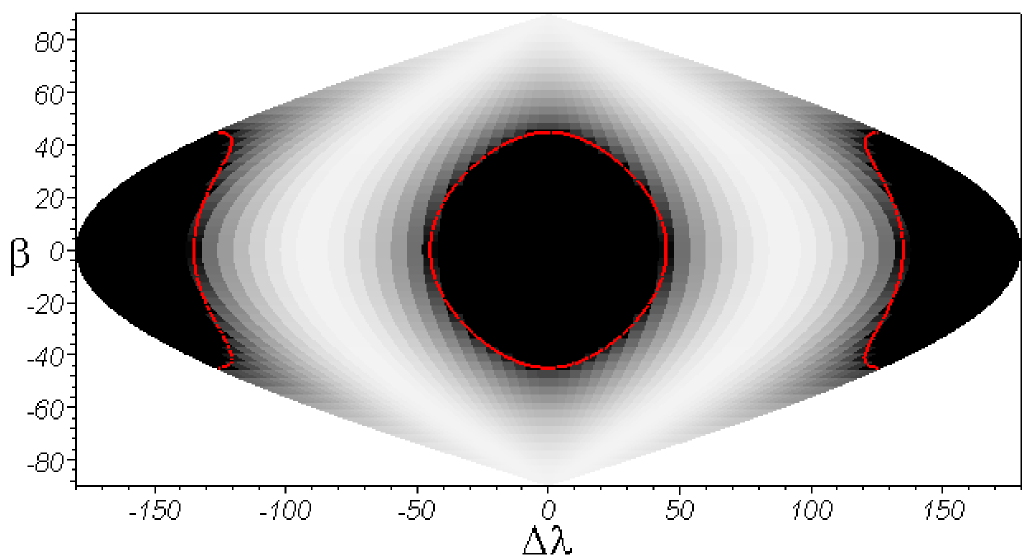

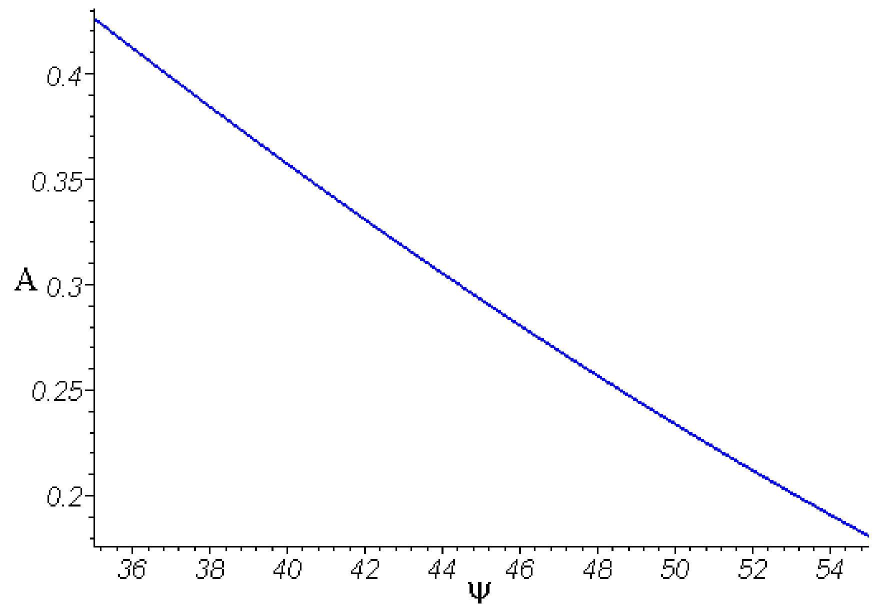

fraction of sky covered by precession cone holes

Geometry *(cont.)*

- Scan angle q as a function of position on the sky
  - longitude coordinate is wrt Sun's ecliptic longitude
- Two solution surfaces
  - due to quadratic solution pair Q
  - smoothly join at discontinuities
- Will smear in longitude due to Earth's orbital motion

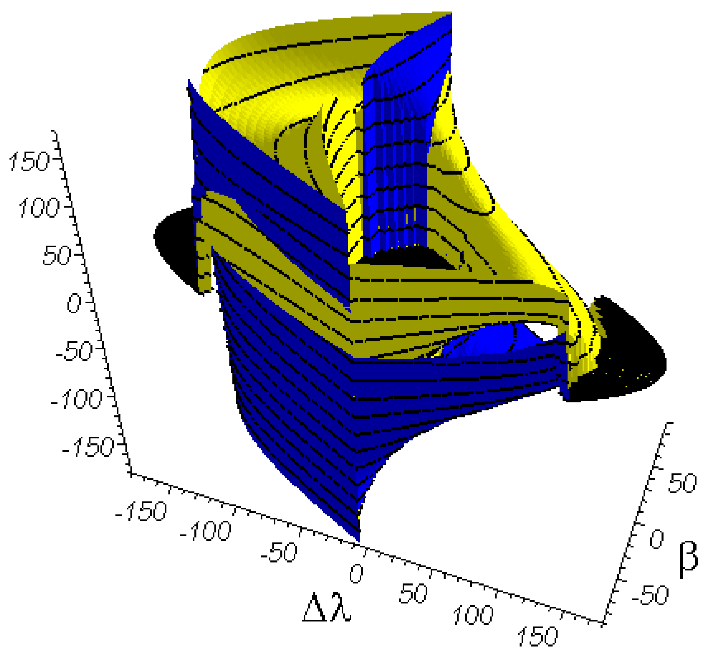

Geometry *(cont.)*

- Fast Euler angle θ as a function of position on the sky
  - longitude coordinate is wrt Sun's ecliptic longitude
- Similarly, two solution surfaces due to Q

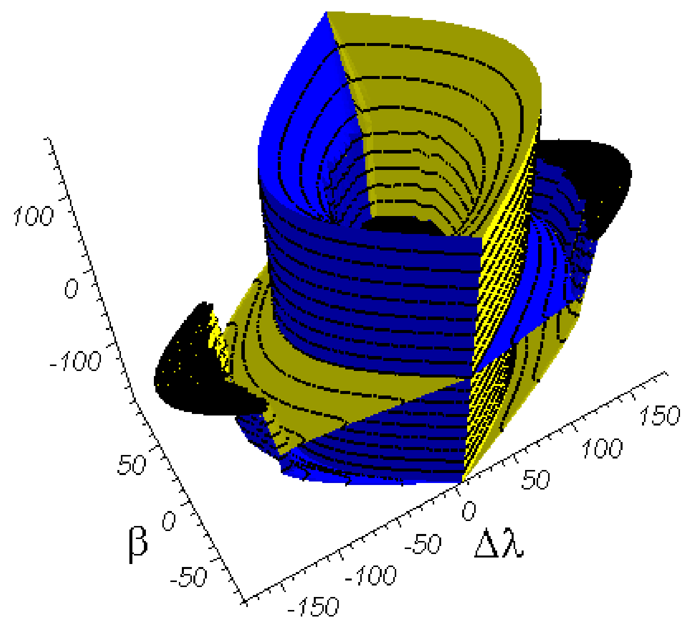

Geometry *(cont.)*

- Slow Euler angle φ (the precession phase angle) as a function of position on the sky
  - longitude coordinate is wrt Sun's ecliptic longitude
- Again, two solution surfaces due to Q

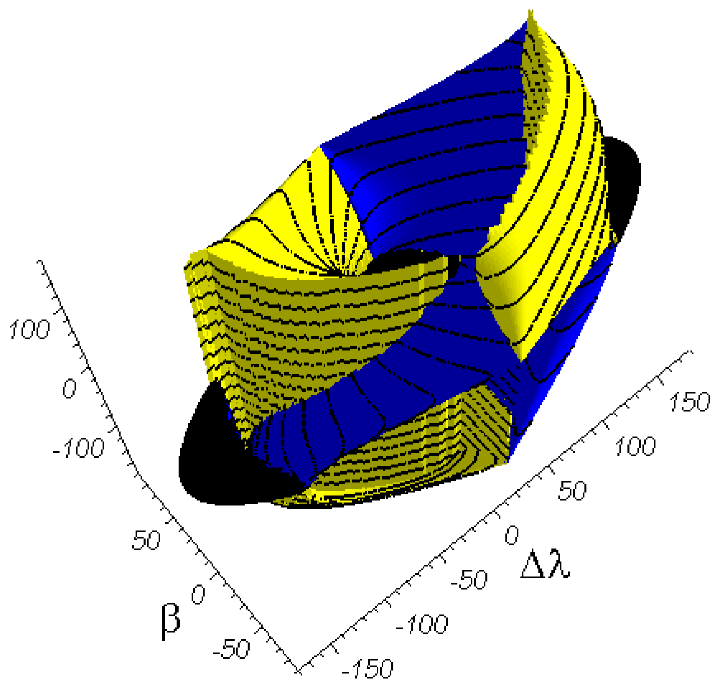

Interlude. The importance of the cross-scan rotation rate

Rotation Rates

- Three orthogonal rotations
  - field rotation
  - cross-scan
  - in-scan $\Omega_s = \frac{d\theta}{dt} + \frac{d\phi}{dt}\cos\psi - Q\cos\beta\frac{d\lambda_S}{dt}$
- Decompose total angular velocity vector along these three rotation axes (which happen to correspond to body-frame [x,y,z], respectively)
- Cross-scan rate
  - determines density of observations on the sky
  - dominated by precession signal
- $\Omega_r = \cos(\lambda-\lambda_S)\cos\beta\frac{d\phi}{dt} + \frac{[\sin^2\psi\sin\beta - Q\cos^2\beta\cos(\lambda-\lambda_S)\cos\psi]\sin(\lambda-\lambda_S)}{\sin\psi\,[Q\sin\beta-\cos\psi\cos(\lambda-\lambda_S)]}\frac{d\psi}{dt} + \sin\beta\frac{d\lambda_S}{dt}$
- $$\begin{aligned}\Omega_c = & -\frac{\cos(\lambda-\lambda_S)\cos\beta}{\sin\psi}\frac{d}{dt}\psi \\ & -\frac{[\sin^2\psi\sin\beta - Q\cos^2\beta\cos(\lambda-\lambda_S)\cos\psi]\sin(-\lambda+\lambda_S)}{Q\sin\beta-\cos\psi\cos(\lambda-\lambda_S)}\frac{d}{dt}\phi \\ & +\left\{\frac{Q^2\cos^2\psi\cos(\lambda-\lambda_S)\sin(-\lambda+\lambda_S)\cos^3\beta}{\sin^2\psi(Q\sin\beta-\cos\psi\cos(\lambda-\lambda_S))}\right. \\ & \quad +\left[-\frac{Q\cos\psi\sin\beta\sin(-\lambda+\lambda_S)}{Q\sin\beta-\cos\psi\cos(\lambda-\lambda_S)}\right. \\ & \quad\quad \left.\left.+\left(-\frac{\cos\psi\cos^2(\lambda-\lambda_S)}{\sin^2\psi}+\frac{Q\sin\beta\cos(\lambda-\lambda_S)}{\sin^2\psi}\right)(\sin(-\lambda+\lambda_S))^{-1}\right]\cos\beta\right\}\frac{d}{dt}\lambda_S\end{aligned}$$

Rotation Rates *(cont.)*

- Cross-scan rate Ω_C as a function of position on the sky
  - longitude coordinate is wrt Sun's ecliptic longitude
- Two solution surfaces due to Q
- Dominated by precession rate term
  - fortunately, an uncomplicated topology
- Ω_C determines the density of observations on the sky
  - **Expect a pile-up of density near the precession cone hole boundaries**
  - Will smear in longitude due to Earth's orbital motion
- plot ordinate axis is scaled by 100 (arcsec/sec)

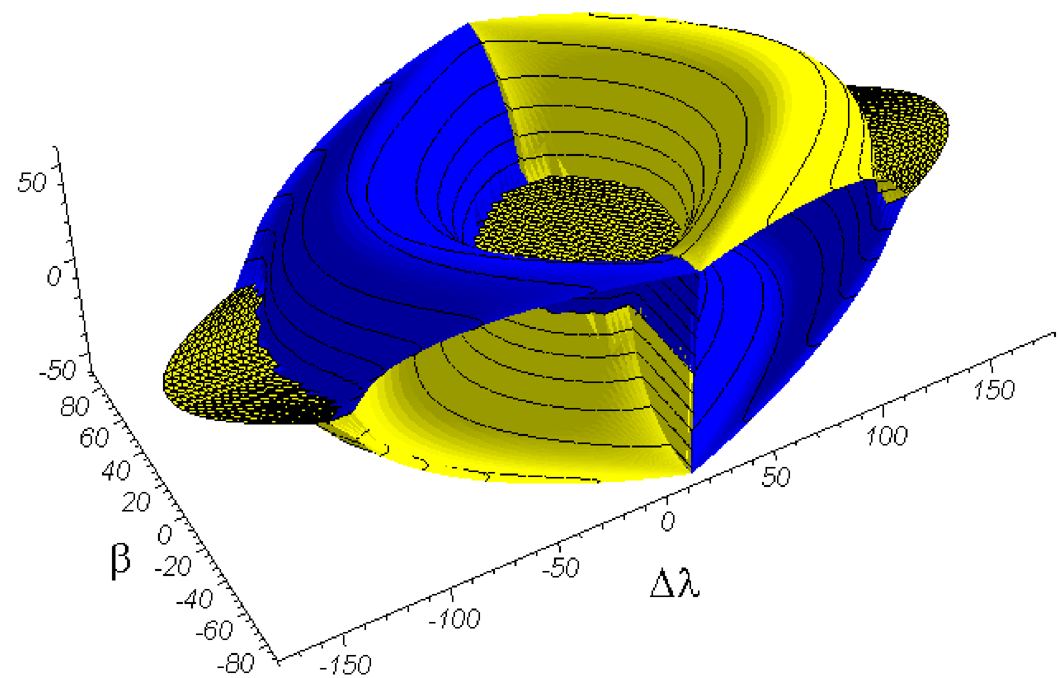

Rotation Rates *(cont.)*

- Observation density on the sky — comoving frame
  - observations every 21 minutes for 1 year
- Notice density enhancement near precession cone hole boundaries
- Use sin β to produce equal-area plot (Lambert cylindrical equal-area)

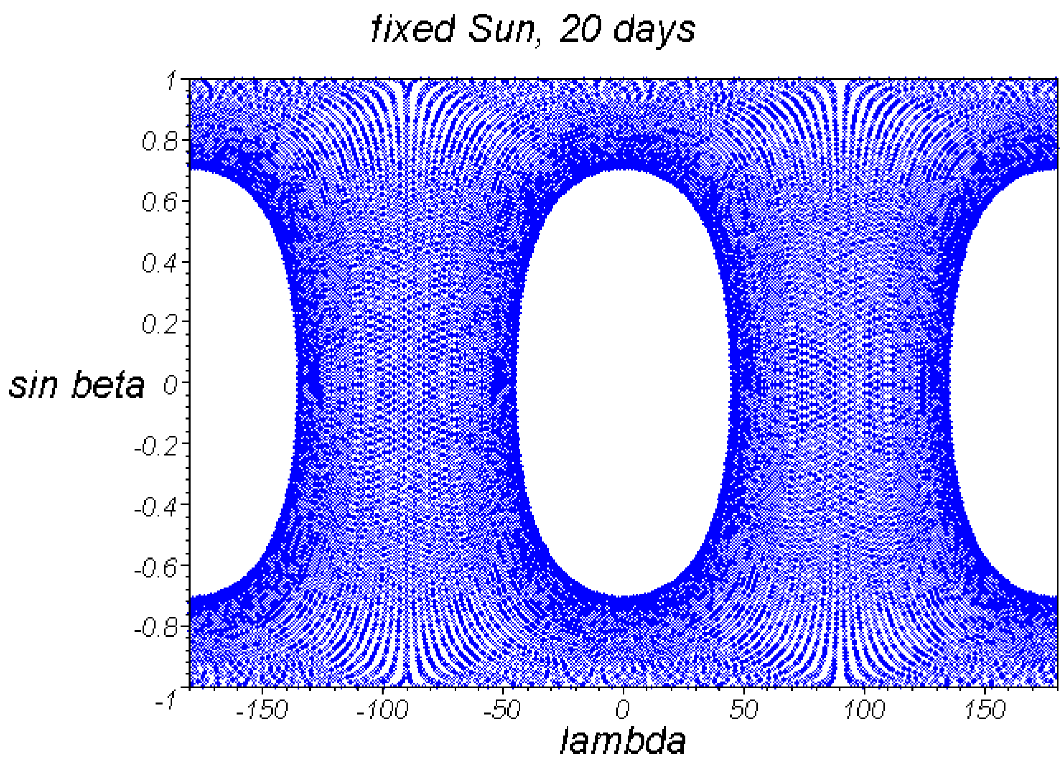

Comments

- Distributions are determined by certain 3D surfaces as functions of ecliptic coordinates
- Sampling on these surfaces as the spacecraft scans the sky creates the two distributions
  - Surface geometry is complicated and very nonuniform (this is bad)
  - Surfaces are slowly smeared in ecliptic longitude as Earth orbits the Sun (this is good)
  - Unfortunately, there is no smearing of the surfaces in ecliptic latitude, so we're stuck with the effects of surface variation as a function of latitude
- Observation density distribution
  - Two zones in latitude where the density peaks
    - Corresponding depression of mean errors
  - Dependence on Sun angle
    - Zones move to higher latitude with smaller Sun angle
    - Zone overdensity increases with smaller Sun angle
  - Dependence on precession period
    - longitudinal inhomogeneity ("ribbing") gets worse with larger precession period

Comments *(cont.)*

- Scan angle distribution (not shown)
  - Large-scale latitude zones (due to precession cone hole effect)
  - Distribution shape:
    - *highly* dependent on sky location
    - ranges from nearly-Gaussian radial profile near poles to *highly* non-Gaussian shape near ecliptic
  - Dependence on Sun angle:
    - Usual high-latitude zone motion
    - Longitudinal inhomogeneities still large after 2.5 years
  - Dependence on precession period:
    - inhomogeneities get worse with larger precession period

Act III. Simulations on an equal-area grid

Simulation Details

- 1-σ scan-direction single-measurement error = 580 μas. This sets the units for the results: μas for parallax and position, and μas/yr for proper motions. Sampled from Gaussian error distribution.
- grid = [341,171], evenly spaced in [longitude, sin latitude]
- Δt = amount of time to scan across one grid cell at equator in longitude direction
  - determined by the grid size specification and the spin period
- spin periods: 35, 40, and 45 minutes
- precession periods: 15, 20, and 30 days
- precession cone angles: 35, 40, and 45 deg
- simulation times: 2.5 years and 5 years
- 2 viewports
- basic angle = 81.5 deg

Simulation Details *(cont.)*

- Observations were performed by between 1 and 4 detectors per viewport. The number of detectors corresponds to the number of astrometric CCDs in one of the 9 CCD columns on the focal plane. The column was chosen randomly for each focal plane crossing of a grid cell.
- astrometric CCD count by column: 123242321
- An option for calculating normal points was available for multiple CCD encounters per focal plane crossing.
- Least squares solutions for the astrometric parameters and their errors were performed for each grid cell. A detailed description of the method is available in the Technical Memorandum, "Astrometric Parameter Estimation Suitable for Simulations", FTM2000-17.
- Sun-tracking variation of Sun angle (~4°) NOT included

Scan Angle Distribution Snapshots

- scatterplots in ecliptic coordinates
  - scale is in milliarcseconds
  - along-scan single-observation errors: Gaussian distribution with 1σ = 0.6 mas

high latitude

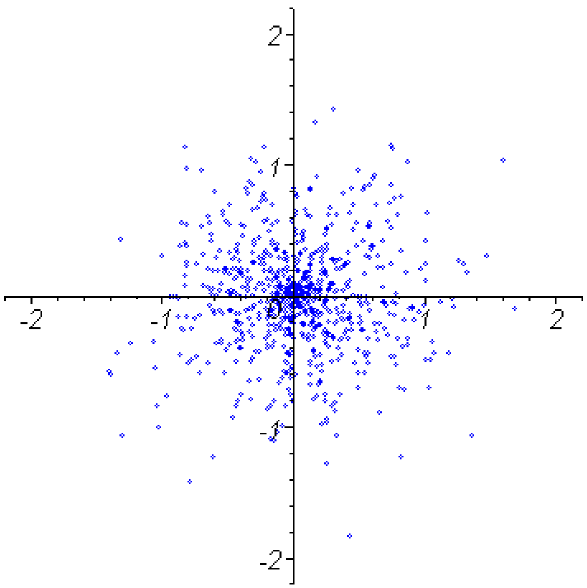

mid-latitude

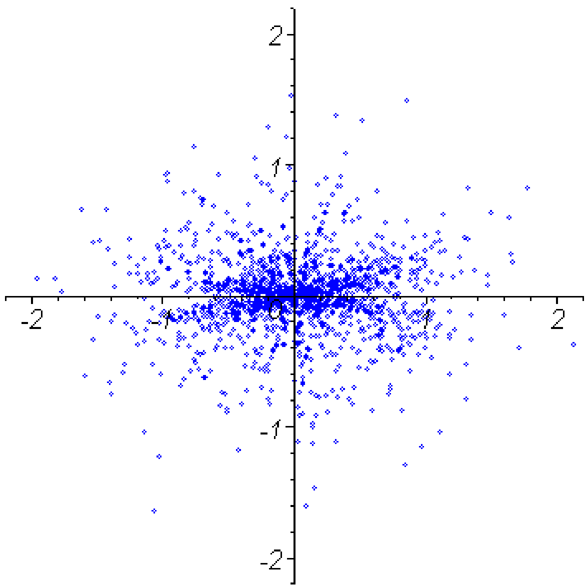

low latitude

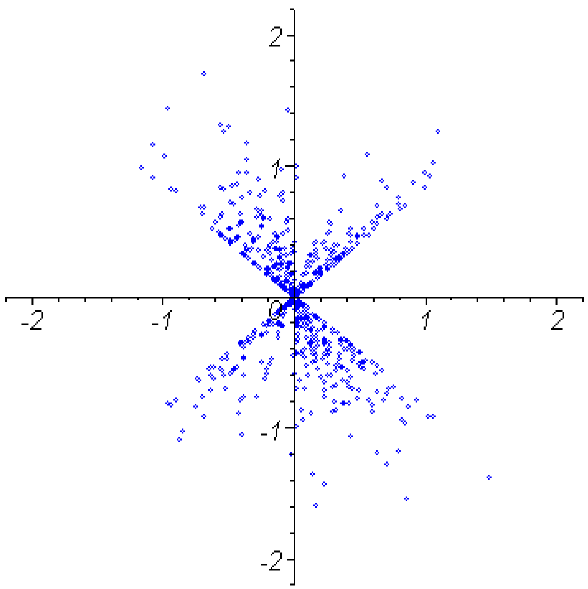

Observation Geometry

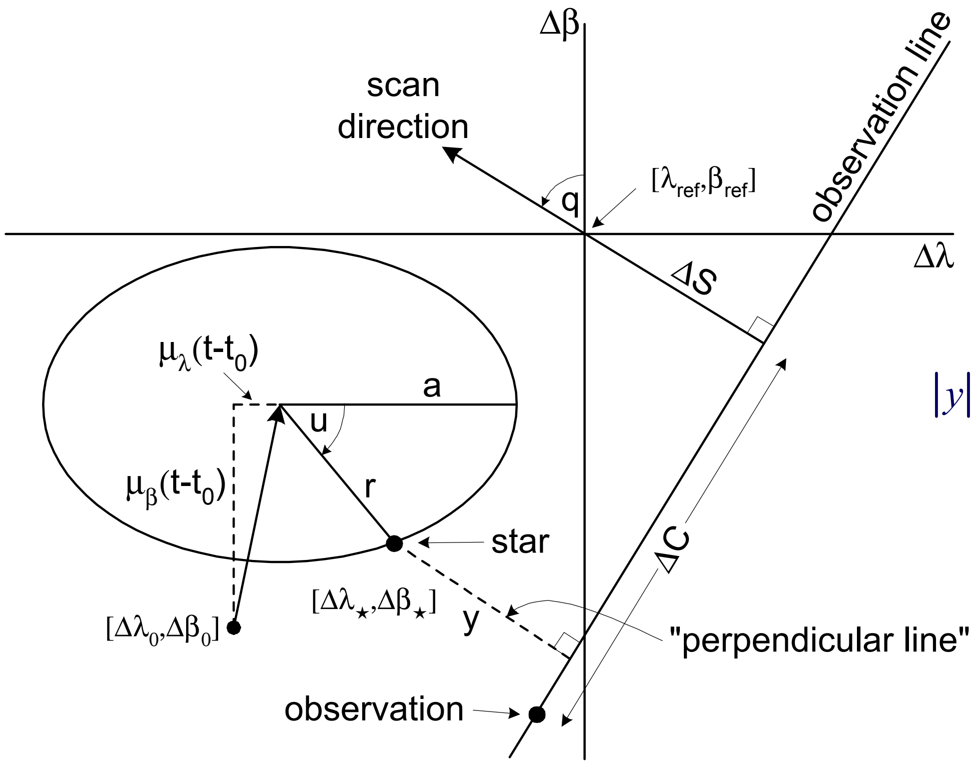

$$
\begin{aligned}
|y| \simeq \quad & \Big| \, \Delta S \\
& - a\left[\sin(\lambda_{ref} - \lambda_{\odot})\sin q + \sin\beta_{ref}\cos(\lambda_{ref} - \lambda_{\odot})\cos q\right] \\
& + \left[\Delta\beta_0 + (t - t_0)\mu_\beta\right]\cos q - \left[\Delta\lambda_0 + (t - t_0)\mu_\lambda\right]\sin q \, \Big|
\end{aligned}
$$

The instrument makes an observation of a star, deriving ΔS and ΔC (scan and cross-scan positions) with respect to local ecliptic coordinates [Δλ,Δβ] located on the sky at [λ_{ref},β_{ref}]. Scan direction is indicated, making an angle *q* wrt the local ecliptic meridian (Δβ axis). The observation point is not coincident with the star due to single-measurement errors. Measurement errors are in general orders of magnitude worse cross-scan than in-scan, causing the measurement error ellipse to be *extremely* elongated. We therefore approximate it as the limiting case: an "observation line". (Note that ΔC is not drawn to scale in the figure.) Given a number of observations, the distance *y* of the observation lines from the true location of the star then becomes the most natural quantity to minimize in a least squares sense.

Due to Earth's orbital motion, the star moves on an ellipse on the sky, with semimajor axis *a* and eccentricity cos β. Due to proper motion [μ_λ,μ_β], the center of the ellipse moves during the mission. The least squares algorithm minimizes the length of the perpendicular line segment *y* by solving for the astrometric parameters: (1) the position [$\Delta\lambda_0$,$\Delta\beta_0$] of the ellipse center at epoch t_0, (2) the proper motion components [μ_λ,μ_β], and (3) the semimajor axis *a* of the parallactic ellipse. The resulting covariance matrix then yields the formal errors and cross-correlations of the parameters.

General Characteristics of the Two Distributions

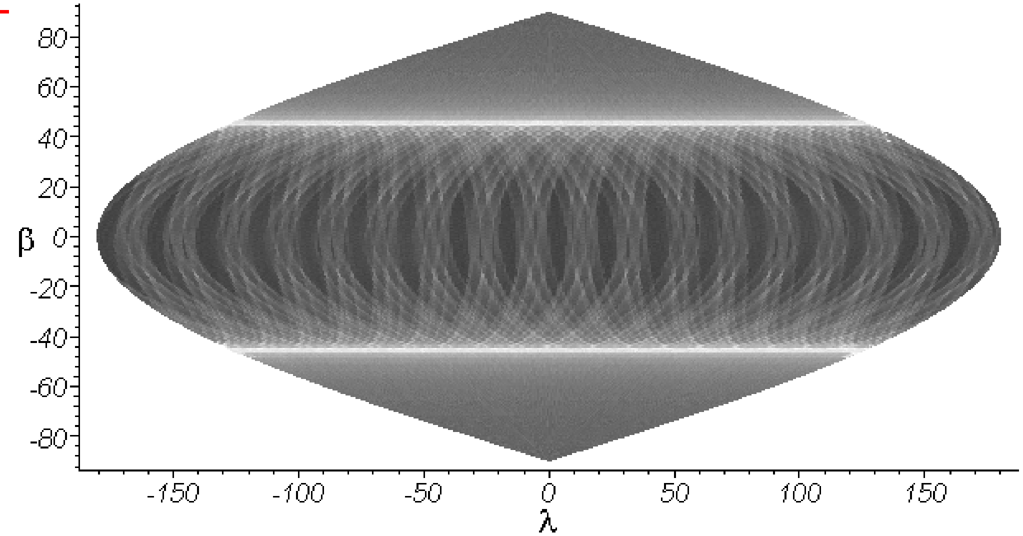

- Observation density distribution
  - highest density at top & bottom of precession cone holes (which smear in longitude), corresponding to two zones in latitude $|\beta| = 90 - \psi$
  - lowest densities are in ecliptic band between the high-density zones
  - ecliptic band exhibits density "ribbing" corresponding to the times when the spacecraft spin axis lies in ecliptic plane
  - ➡ best accuracies should be in the mid-latitude high-density zones
  - ➡ worst accuracies should be in the ecliptic band
  - ➡ ecliptic band is not uniformly bad
- Scan angle distribution
  - homogeneous in polar cap regions (latitudes above high-density zones)
  - cone-shaped on ecliptic, with cone opening angle $90 - \psi$
  - ➡ better position accuracies in polar cap regions
  - ➡ longitude position accuracy substantially degraded near ecliptic
  - ➡ latitude position accuracy slightly degraded near ecliptic
  - ➡ better parallax accuracy in polar cap regions

All-Sky Error Distributions (45 deg. Sun Angle)

errors in parallax
(log scaling)

errors in longitude

errors in latitude

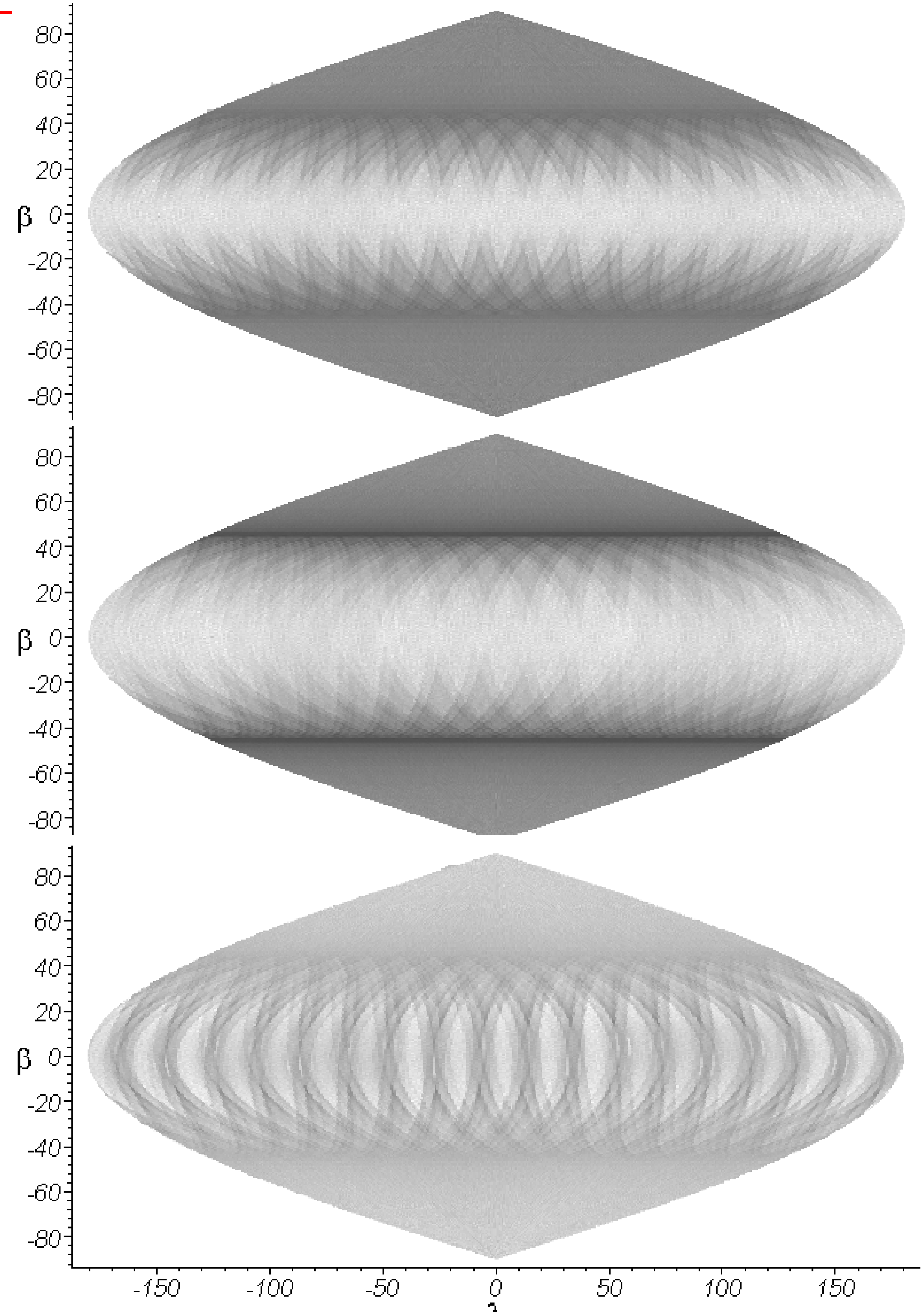

Components of Histograms and their Behavior

- sky naturally divided by scanning geometry into distinct regions:
  - high-density troughs at $|\beta| = 90 - \psi$
  - ecliptic band $|\beta| < 90 - \psi$
  - polar caps $|\beta| > 90 - \psi$
- as Sun angle decreases:
  - polar caps shrink
  - ecliptic band grows
  - longitude
    - high-accuracy population shrinks, moves left
    - low-accuracy population grows, moves right
  - latitude
    - distribution broadens and peak moves left
  - parallax
    - main feature shrinks, moves left
    - poor-accuracy fraction grows

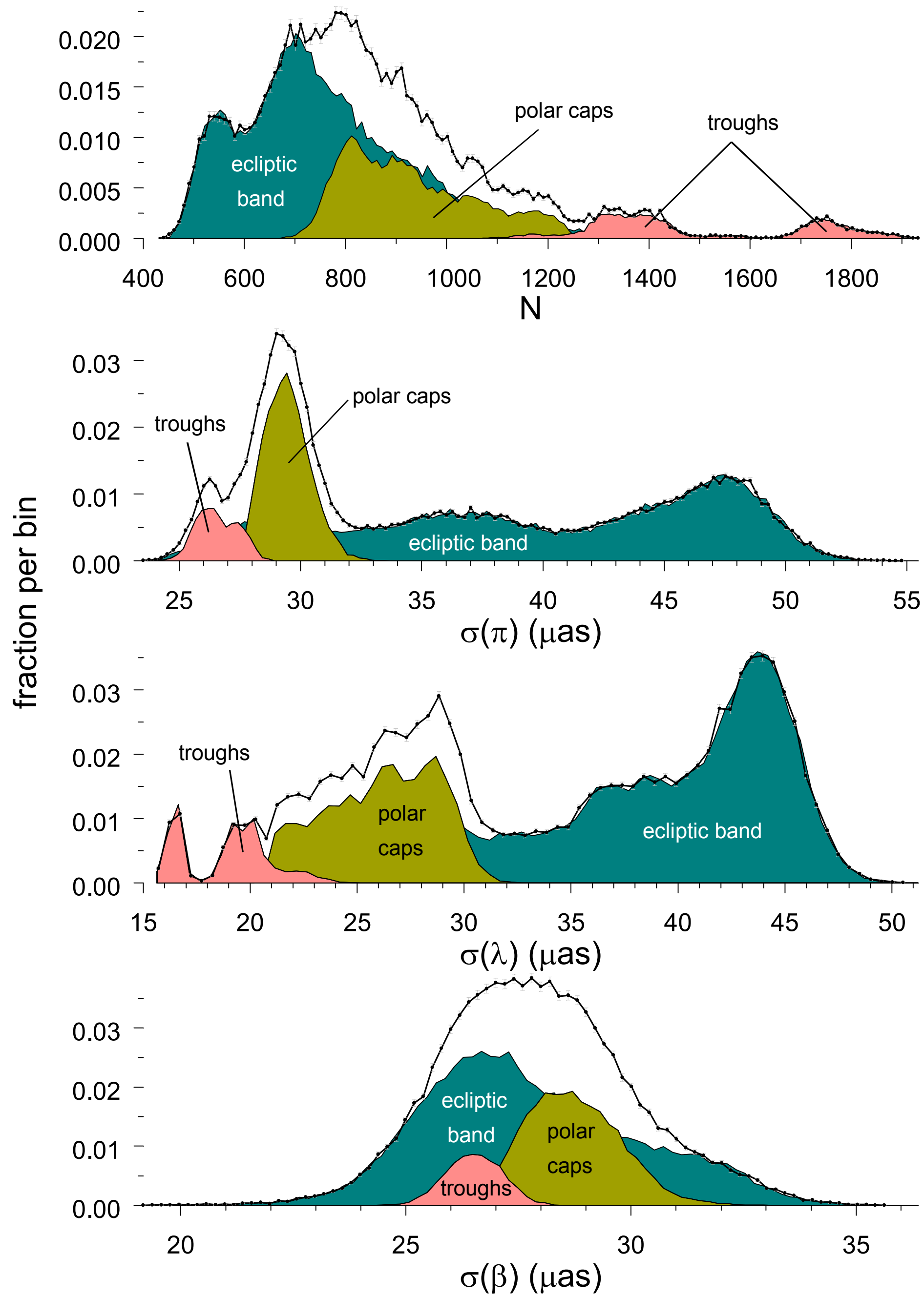

Part 1. Variation of precession cone angle

Histograms: Observation Counts

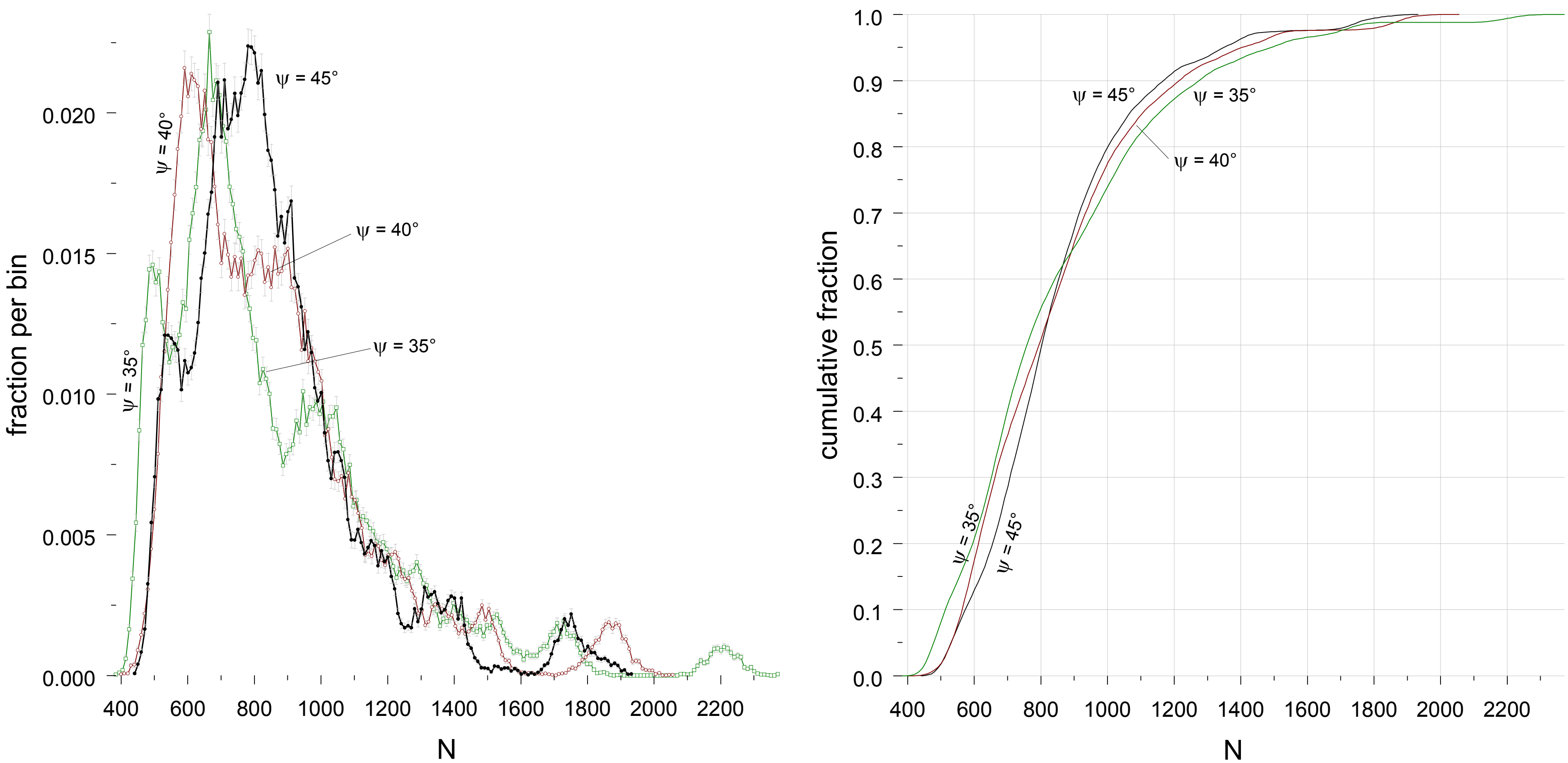

Histograms: Errors in Parallax

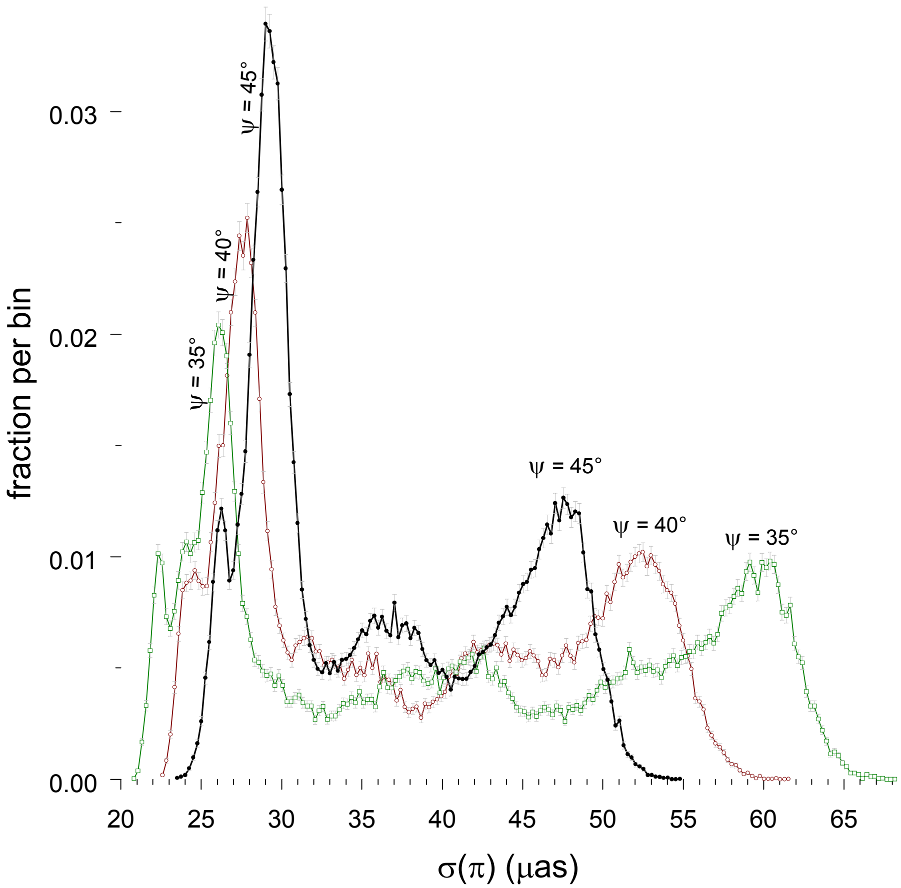

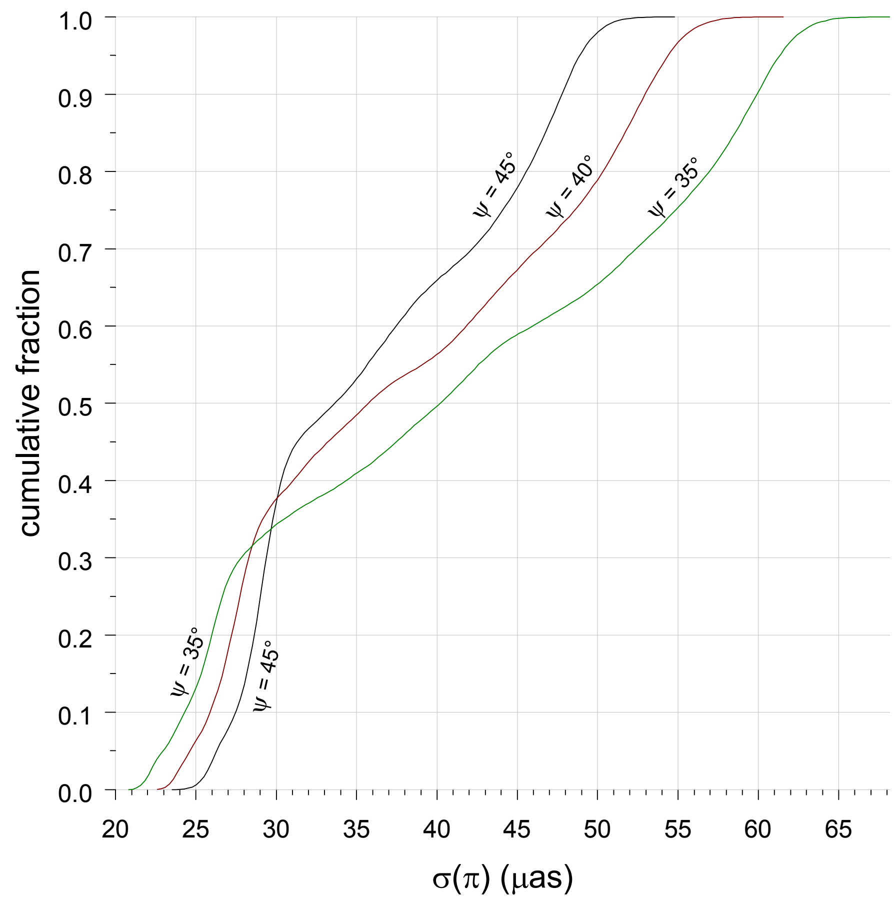

Histograms: Errors in Ecliptic Longitude

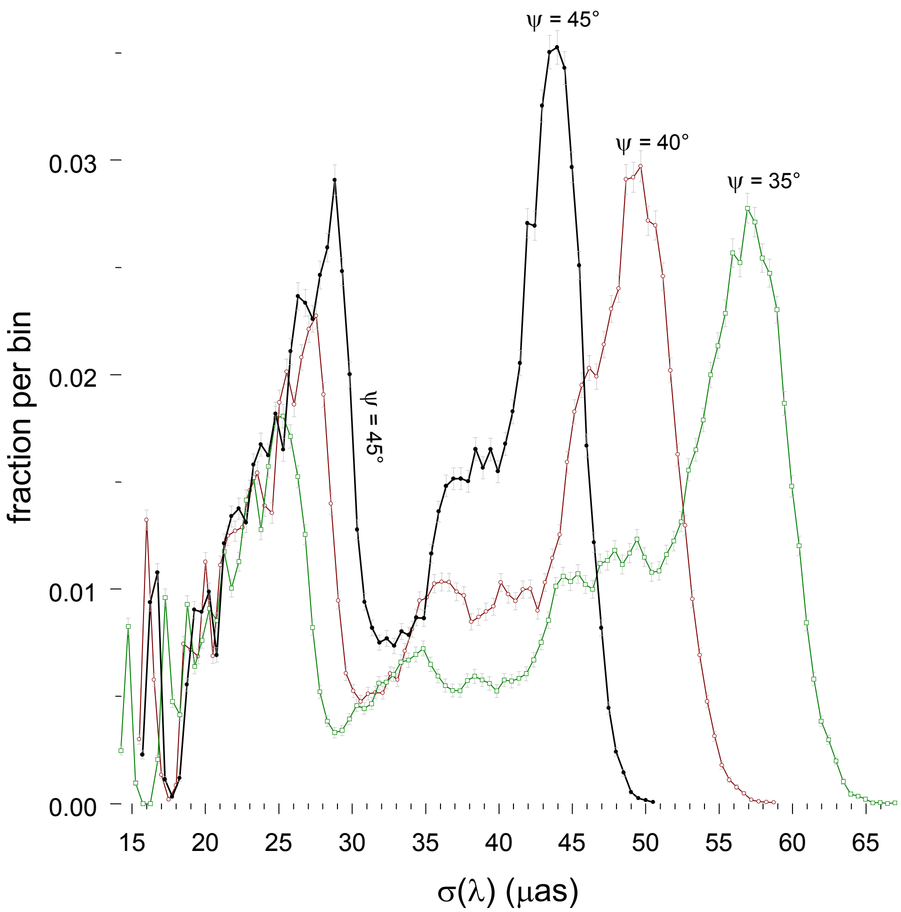

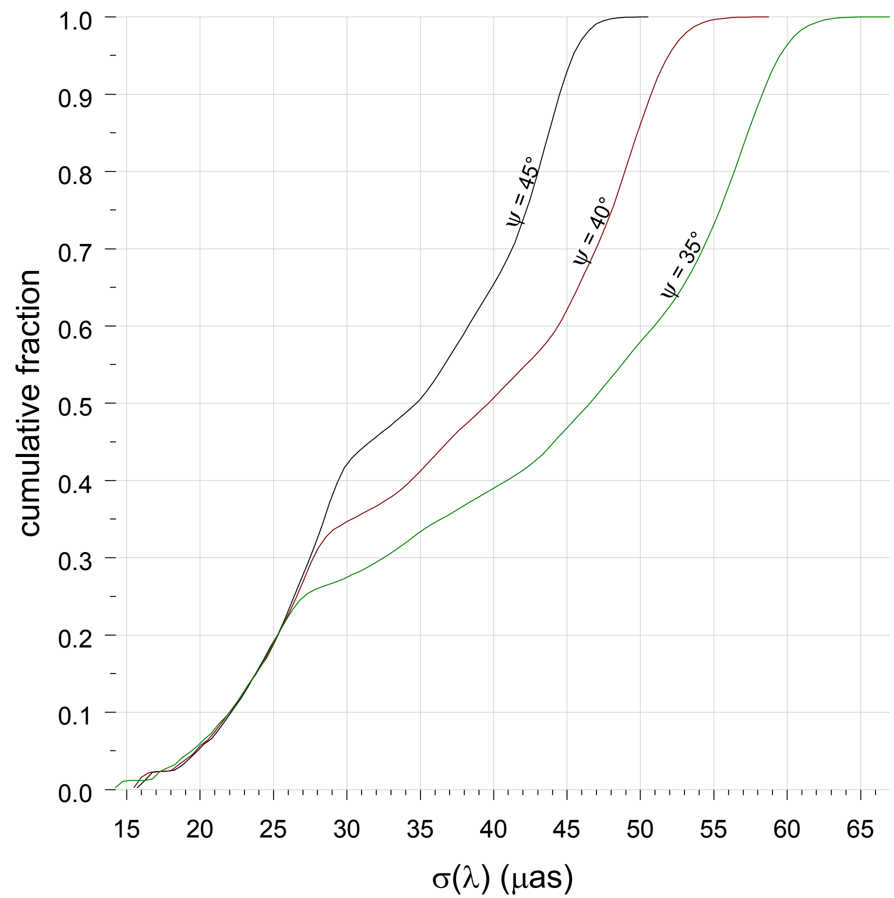

Histograms: Errors in Ecliptic Latitude

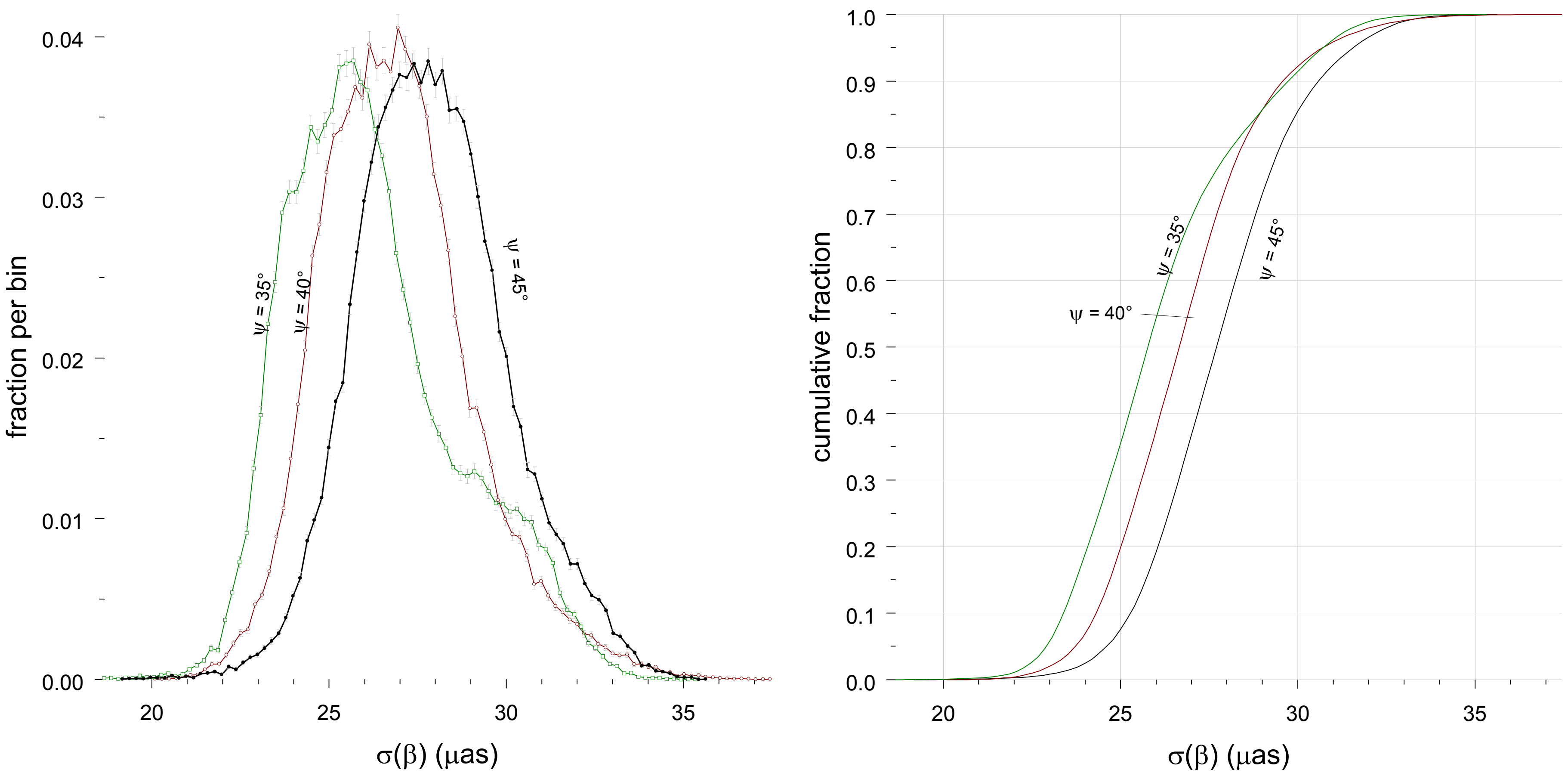

Histograms: Errors in Proper Motion in Longitude

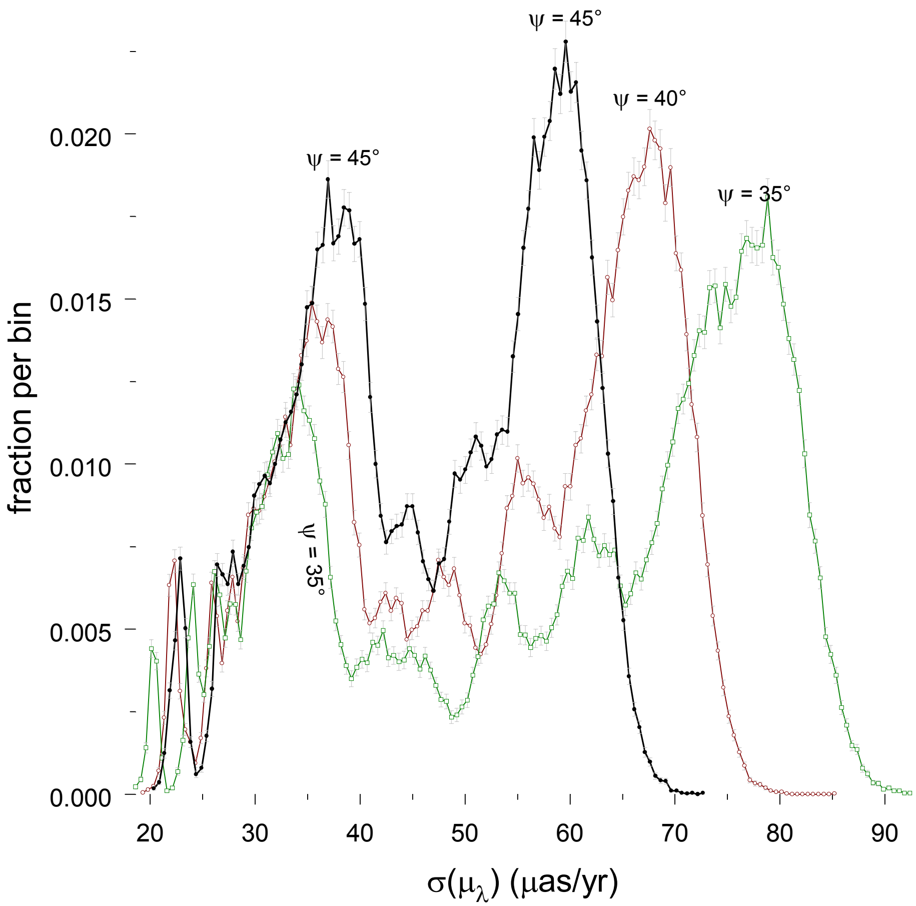

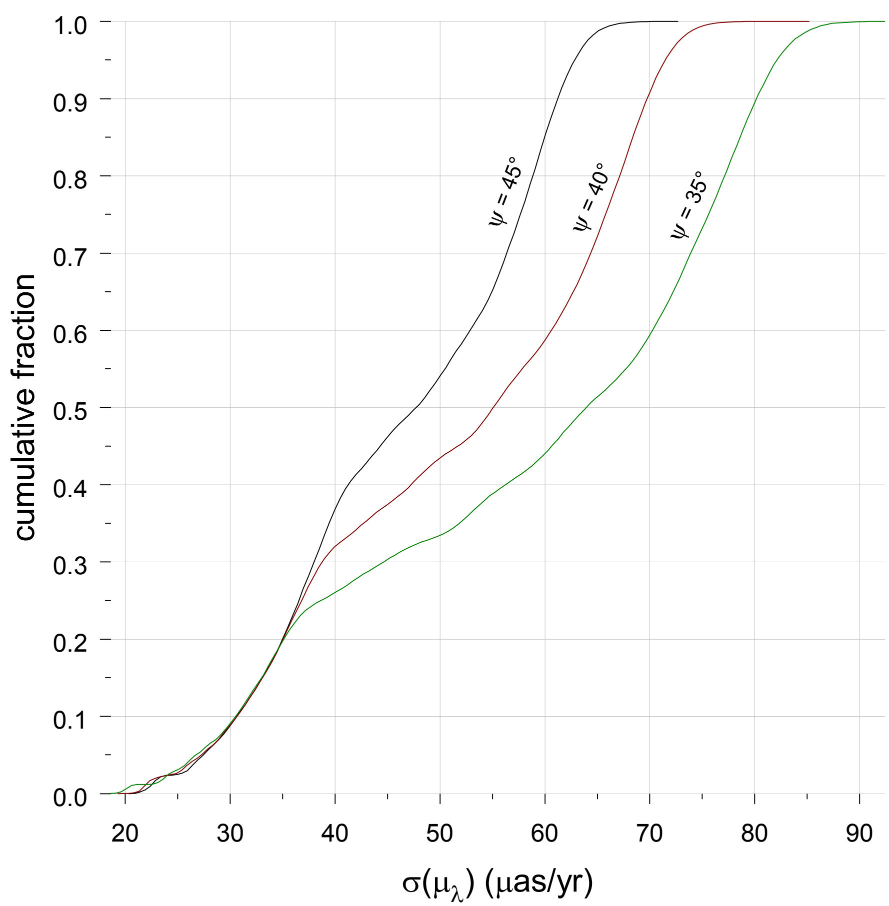

Histograms: Errors in Proper Motion in Latitude

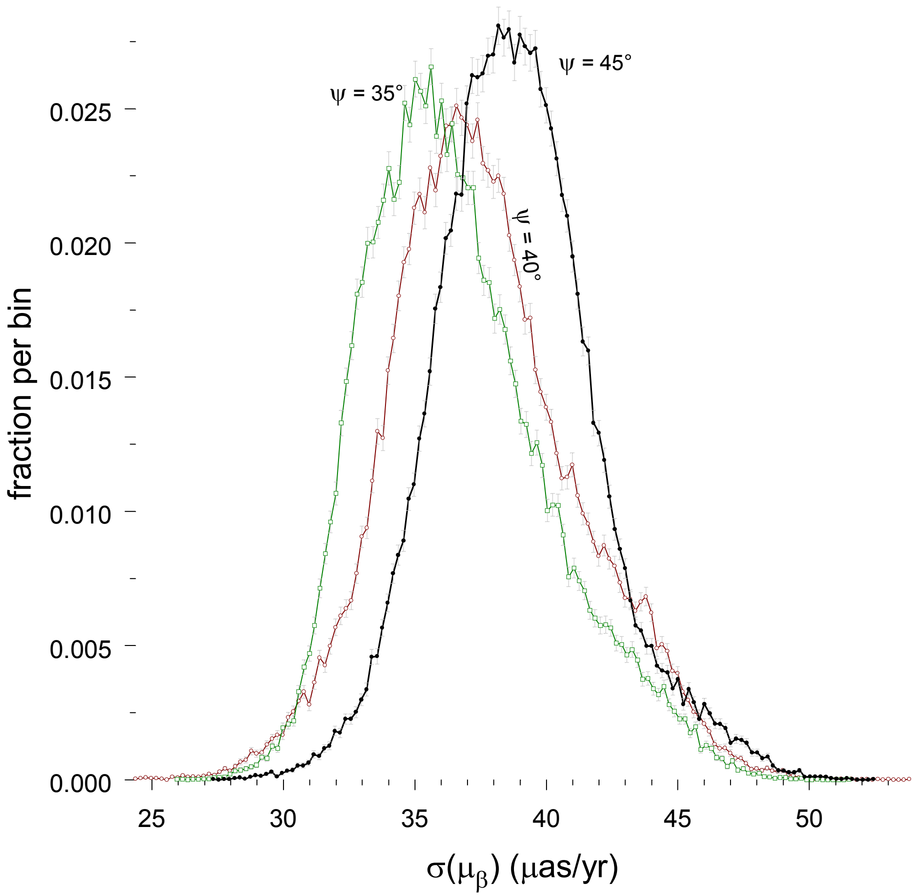

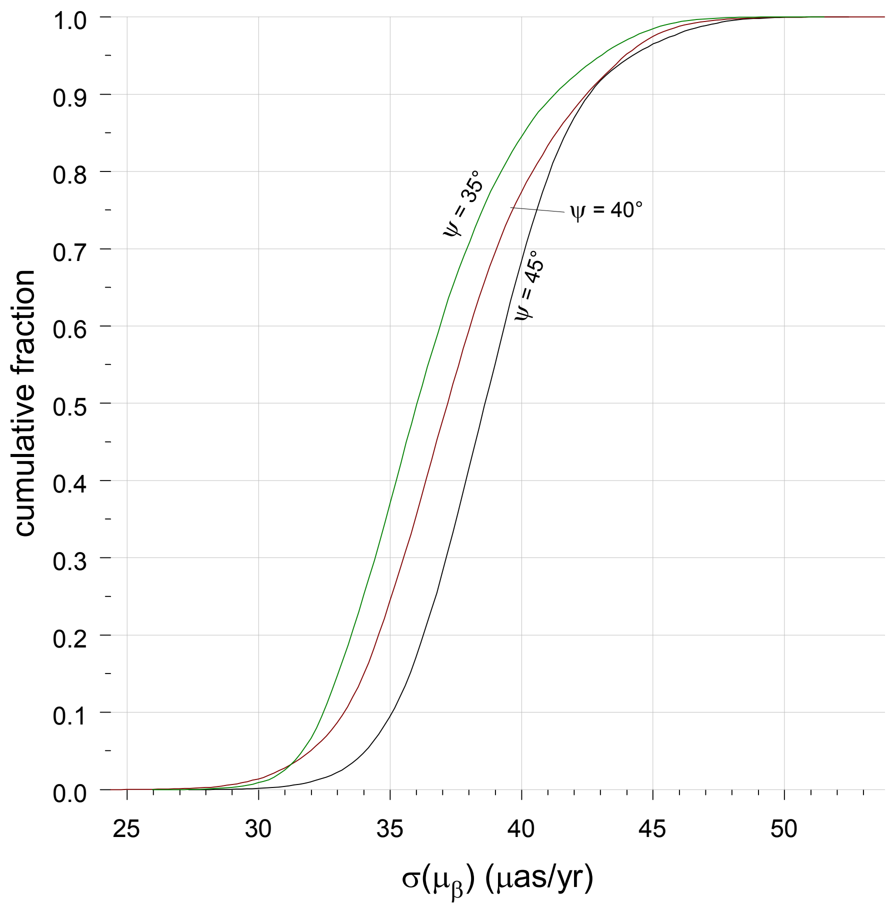

Median Values

- Medians of longitude bands as function of latitude

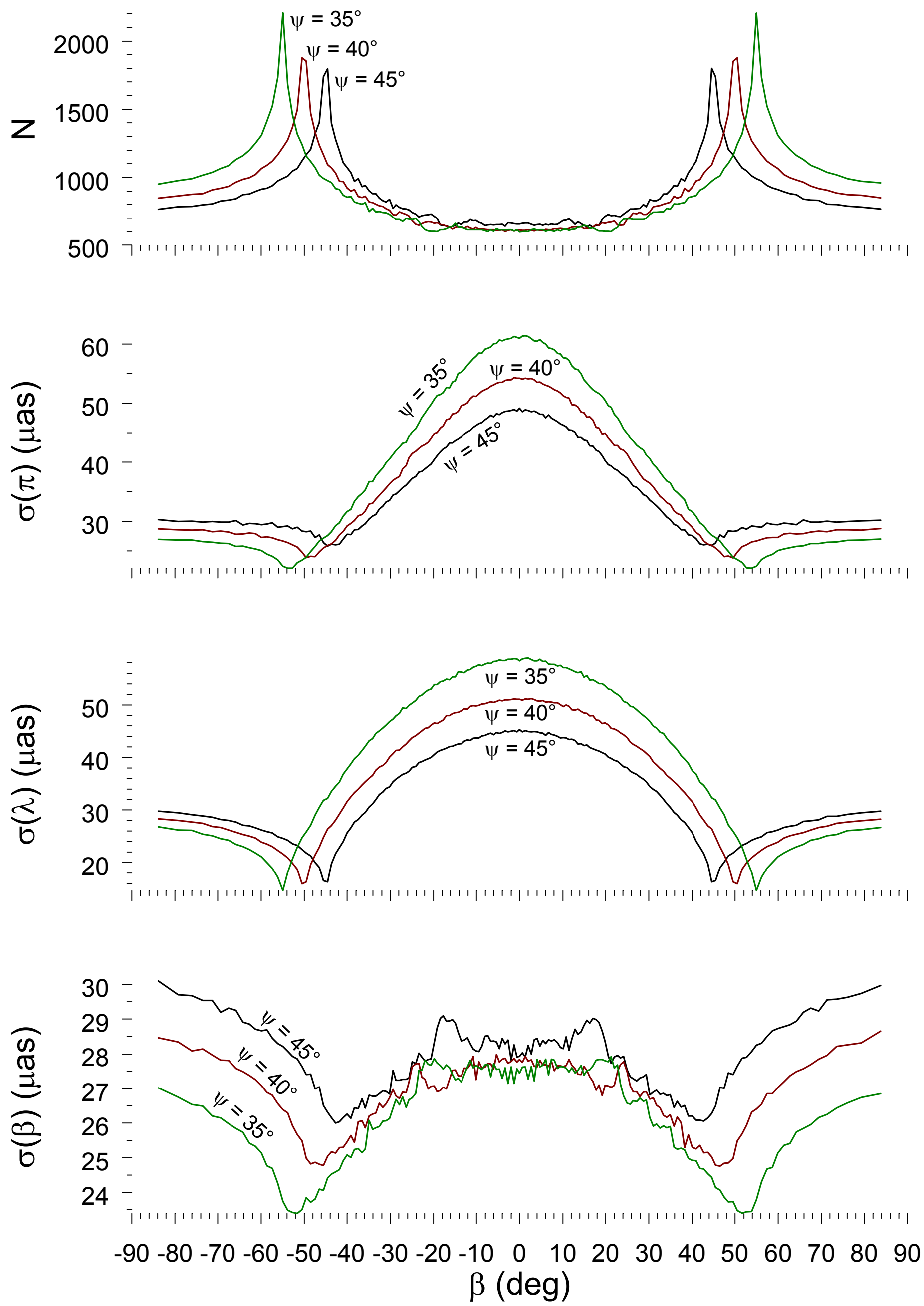

Comments

- Three cases are shown for precession cone angles (i.e., nominal Sun angles) of 35, 40, and 45 degrees. Larger than 45 degrees runs into trouble with shield size (hardware complexity and cost, in addition to increase of perturbations). Smaller than 35 degrees and we won't meet the (most likely definition of the) mission requirements.
- In general, the mission astrometric errors degrade as the nominal Sun angle decreases.
- We do very well in latitude errors: histogram peaks are around 26-28 uas, and 100 percent of the sky is better than 37 μas even for the worst case. Hence, with respect to latitude errors, mission requirements are not affected by nominal Sun angle in the range 35-45 degrees.
- Nearly 100 percent of the sky is 50 μas or better in both longitude (99.99%) and parallax (98.1%) for the 45 degree case. Going to 40 degrees costs us about 18 percent of the sky at 50 μas in parallax, and it costs about 14 percent of the sky at 50 μas in position in longitude. At 35 degrees nominal Sun angle the requirement of 90 percent of the sky at 50 μas or better is not met.

Comments *(cont.)*

- However, even at 35 degrees, the worst parallax error is only 69 μas and the worst longitude error is only 67 μas.
- Proper motion in longitude significantly fails the 90 percent of the sky, <50 μas/yr target for all three precession cone angles.
- The parallax requirement of 90 percent of the sky better than 50 μas restricts the precession cone angle to greater than or equal to 43 degrees.
- Ratios of errors in the ecliptic region to those in the polar regions get substantially worse for longitude and parallax as you decrease the nominal Sun angle from 45 degrees to 35 degrees. The corresponding ratios get slightly better for errors in latitude, but the difference is so small as to not matter.
- The observation count is roughly in the range 600-1000 for most areas of the sky. The dominant histogram peak shifts towards lower counts as the precession cone angle decreases.

Comments (cont.)

- A test was run during which normal points were simulated whenever more than one CCD was encountered during a focal plane crossing. In such cases, the weight of the observation was proportional to the number of CCDs in the given column. There was almost no difference in the resulting astrometric error distributions.
- The FAME observation density distribution is much more uniform than that of HIPPARCOS, especially with a 5-year extended mission. It is, however, affected by changes in the precession period.

Comments *(cont.)*

- The table below shows percentages of the sky for which a 2.5 year FAME mission can meet or do better than the goals of 50 μas (position, parallax) and 50 μas/yr (proper motion), for three nominal Sun angles and assuming a 580 uas single-measurement standard error.

	45 degrees	40 degrees	35 degrees
parallax	98	79	65
position — longitude	100	86	58
position — latitude	100	100	100
pm — longitude	54	43	33
pm — latitude	100	100	100

Part 2. Variation of spin period

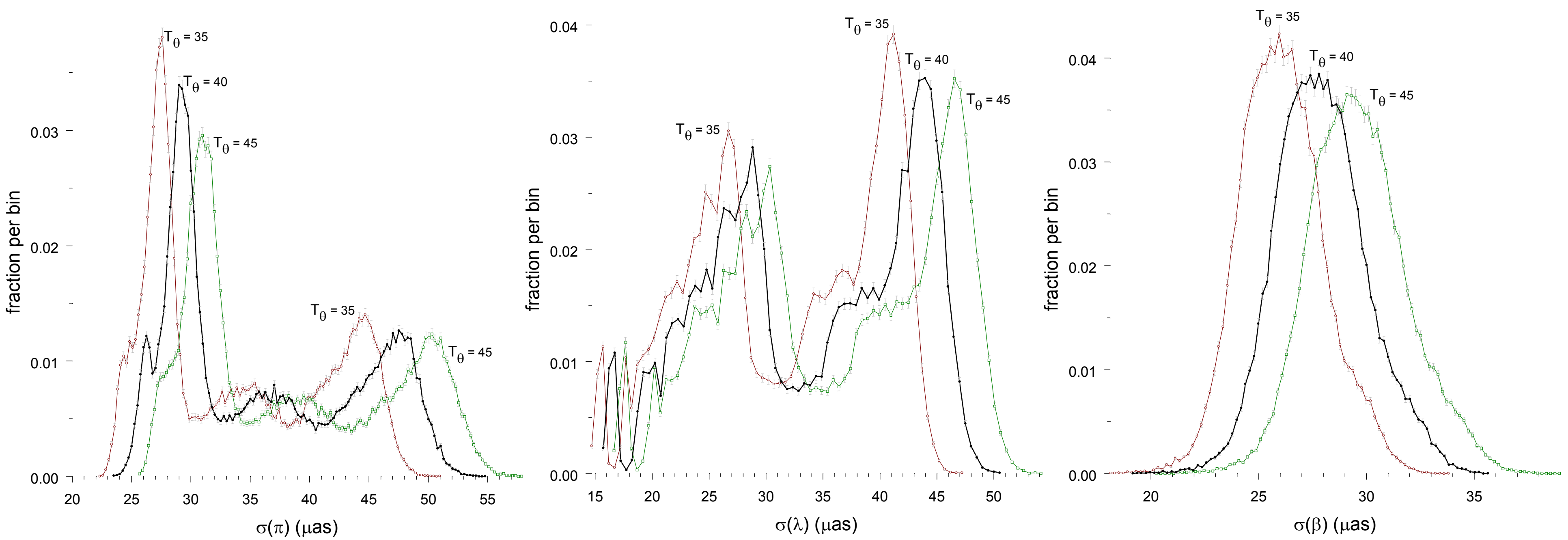

fraction per bin
σ(π) (μas)
σ(λ) (μas)
σ(β) (μas)
Tθ = 35
Tθ = 40
Tθ = 45

Comments

- The following table shows minimum, median, average, and maximum values. Units are μas and μas/yr.

	35 minutes	40 minutes	45 minutes
parallax	100	98	86
position — longitude	100	100	98
position — latitude	100	100	100
pm — longitude	62	54	48
pm — latitude	100	100	98

Comments *(cont.)*

- Variation of Spin Period
  - There is almost no discernible difference in the structure of the observation density distribution as the spin period changes, at least in the range 35 to 45 minutes. The density scales uniformly as a function of the spin period.
  - In general, the mission astrometric errors degrade as the spin period increases.
  - Proper motion in longitude significantly fails the 90 percent of the sky, <50 μas/yr target for all three spin periods.
  - The parallax requirement of 90 percent of the sky better than 50 μas restricts the spin period to less than or equal to 43 minutes.

Part 3. Variation of precession period

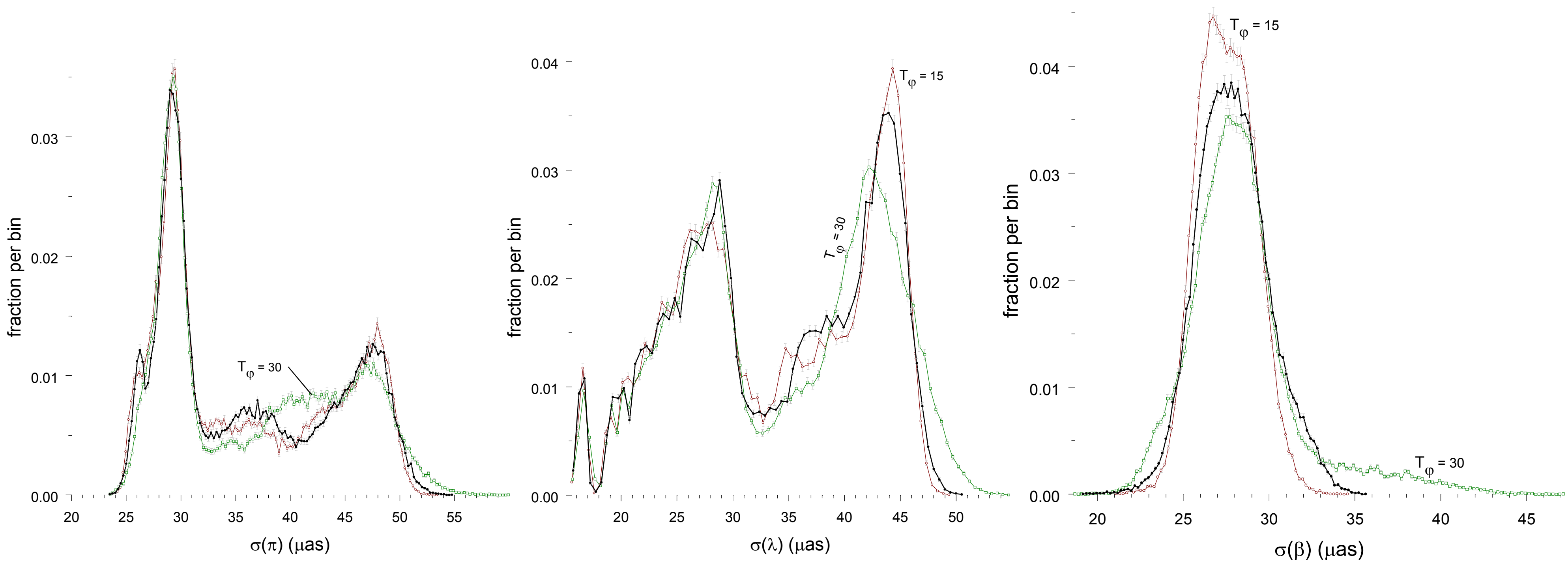
fraction per bin
0.00
0.01
0.02
0.03
20
25
30
35
40
45
50
55
σ(π) (μas)
Tφ = 30
0.04
σ(λ) (μas)
Tφ = 15
σ(β) (μas)

Comments

- Variation of Precession Period
  - The structure of the observation density distribution on the sky is sensitive to the precession period. Coverage is more uniform for smaller precession periods.
  - However, there is almost no difference in the mission astrometric errors for precession periods in the range 15 to 30 days.
  - Results begin to deteriorate around 30 days, which therefore probably represents a reasonable upper bound on the precession period.

Part 4. A 5-year mission

5-Year Observation Density Distribution

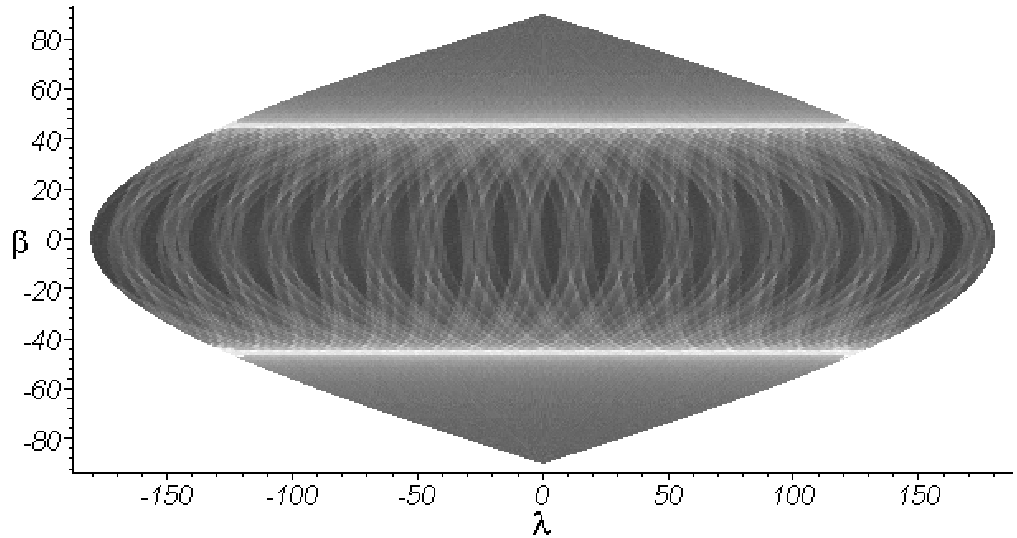

2.5 years

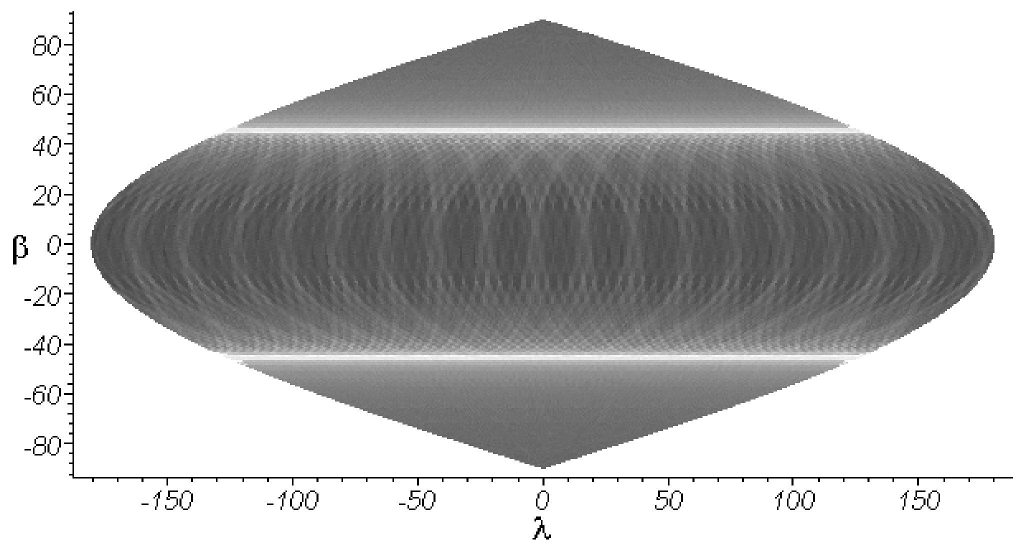

5 years

5-Year Mission Histograms

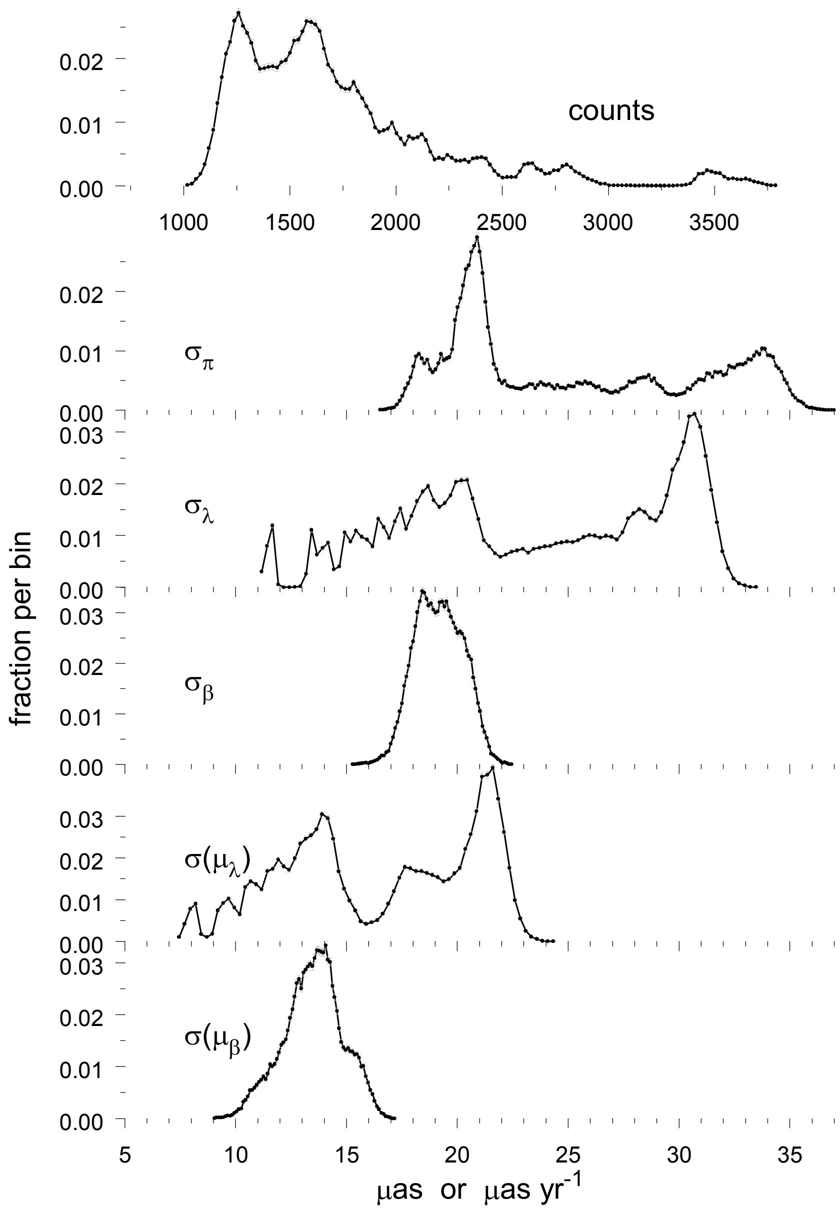

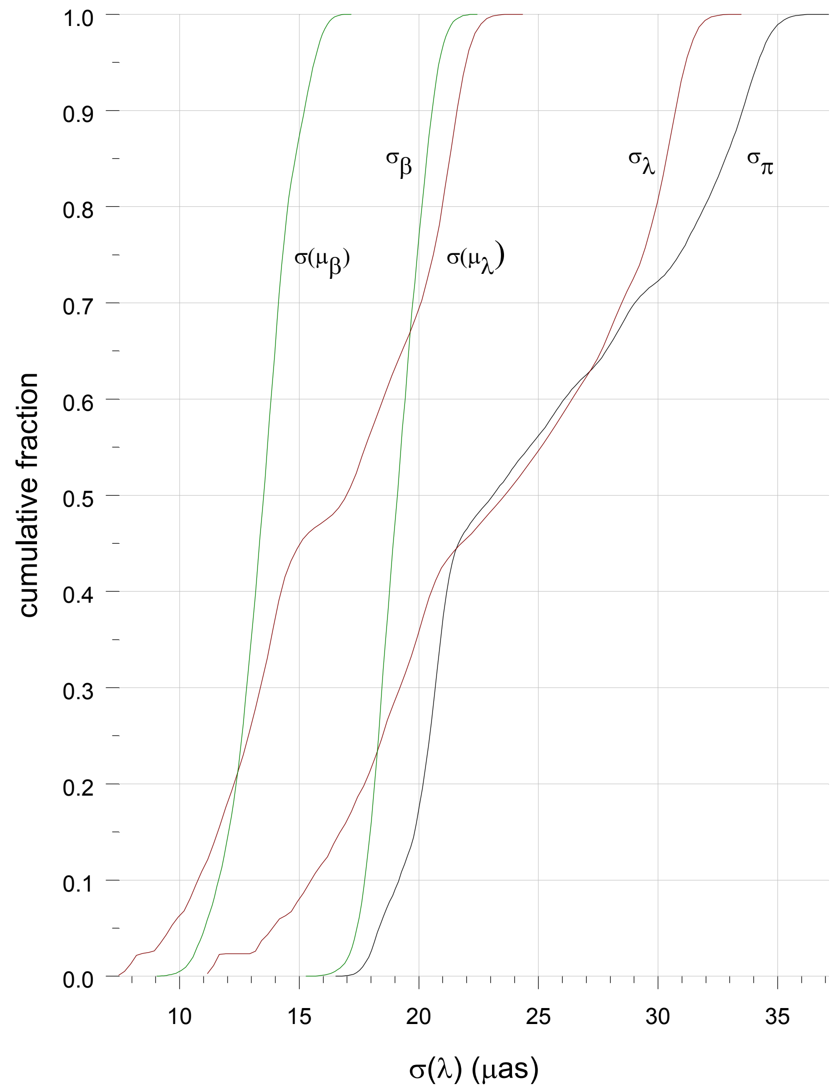

.

Comments

- 5-Year Extended Mission
  - The observation density is smoother -- longitudinal ribbing effect is lessened (compare the observation density all-sky image of the 2.5-year case to that of the 5-year case).
  - All errors fall well within the 50 uas or μas/yr mission requirements.
  - Position in latitude and both proper motion components are entirely less than 25 μas or μas/yr.
  - The polar cap parallax feature is at about 21 μas.

Hipparcos